Geoscience Frontiers 14 (2023) 101518

Contents lists available at ScienceDirect

Geoscience Frontiers

journal homepage: www.elsevier.com/locate/gsf

Research Paper

The Holocene environmental changes revealed from the sediments of the Yarkov sub-basin of Lake Chany, south-western Siberia

S.K. Krivonogov [a,b,c,*], A.N. Zhdanova [a], P.A. Solotchin [a], A.Y. Kazansky [d,e], V.V. Chegis [f], Z. Liu [g,h], M. Song [g], S.V. Zhilich [i], N.A. Rudaya [i,j], X. Cao [k], O.V. Palagushkina [l], L.B. Nazarova [l,m], L.S. Syrykh [n]

[a] Institute of Geology and Mineralogy, Russian Academy of Sciences, Siberian Branch, Novosibirsk, Russia
[b] Novosibirsk State University, Novosibirsk, Russia
[c] Korkyt Ata Kyzylorda University, Kyzylorda, Kazakhstan
[d] Moscow State University, Moscow, Russia
[e] Geological Institute, Russian Academy of Sciences, Moscow, Russia
[f] Pushkov Institute of Terrestrial Magnetism, Ionosphere and Radio Wave Propagation, Russian Academy of Sciences, Troitsk, Russia
[g] Department of Earth Sciences, The University of Hong Kong, Hong Kong, China
[h] State Key Laboratory of Loess and Quaternary Geology, Institute of Earth Environment, Chinese Academy of Sciences, Xi'an, China
[i] Institute of Archaeology and Ethnography, Russian Academy of Sciences, Siberian Branch, Novosibirsk, Russia
[j] Tomsk State University, Tomsk, Russia
[k] Alpine Paleoecology and Human Adaptation Group (ALPHA), State Key Laboratory of Tibetan Plateau Earth System, Environment and Resources (TPESER), Institute of Tibetan Plateau Research, Chinese Academy of Sciences, Beijing, China
[l] Volga Region Federal University, Kazan, Russia
[m] Krasnoyarsk Science Center, Russian Academy of Sciences, Siberian Branch, Krasnoyarsk, Russia
[n] Herzen State Pedagogical University, St. Petersburg, Russia

ARTICLE INFO

Article history:
Received 11 April 2022
Revised 16 October 2022
Accepted 23 November 2022
Available online 29 November 2022
Handling Editor: Vinod Samuel

Keywords:
Saline lake
Multiproxy study
Holocene
Climate
Environment
West Siberia

ABSTRACT

Lake Chany is the largest endorheic lake in Siberia whose catchment is entirely on the territory of Russia. Its geographical location on the climate-sensitive boundary of wet and dry landscapes provides an opportunity to gain more knowledge about environmental changes in the West Siberian interior during the Holocene and about the evolution of the lake itself. Sediment cores obtained from the Yarkov sub-basin of the lake in 2008 have been comprehensively studied by a number of approaches including sedimentology and AMS dating, pollen, diatom and chironomid analyses (with statistical interpretation of the results), mineralogy of authigenic minerals and geochemistry of plant lipids (biomarker analysis.). Synthesis of new results presented here and published data provides a good justification for our hypothesis that Lake Chany is very young, no older than 3.6 ka BP. Before that, between 9 and 3.6 ka BP, the Chany basin was a swampy landscape with a very low sedimentation rate; it could not be identified as a water body. In the early lake phase, between 3.6 and 1.5 ka BP, the lake was shallow, 1.2–3.5 m in depth, and it rose to its modern size, up to 6.5 m in depth, during the last millennium. Our data reveal important changes in the understanding of the history of this large endorheic lake, as before it was envisioned as a large lake with significant changes in water level since ca. 14 ka BP. In addition to hydrology, our proxies provide updates and details of the regional vegetation and climate change since ca. 4 ka BP in the West-Siberian forest-steppe and steppe. As evolution of the Chany basin is dependent on hydroclimatic changes in a large region of southern West Siberia, we compare lake-level change and climate-change proxies from the other recently and most comprehensively studied lakes of the region.

1. Introduction

Inner Eurasia holds a number of topography-related closed lakes located on vast interfluve flatlands. Those situated in the semiarid and arid climatic zones are saline due to intensive evaporation of precipitation and run-off into the lakes from their

* Corresponding author at: Institute of Geology and Mineralogy, Russian Academy of Sciences, Siberian Branch, Novosibirsk, Russia.
E-mail address: carpos@igm.nsc.ru (S.K. Krivonogov).

https://doi.org/10.1016/j.gsf.2022.101518
1674-9871/

catchments. Such endorheic lakes are highly sensitive to climate change in terms of moisture supply and solar radiation, resulting in frequent and profound fluctuations in lake water levels, which are well documented in historical records and sediment archives. Researchers draw attention to this type of lakes because of their high academic and practical value; many large lakes of Central Asia and Southern Siberia are studied (e.g. Tarasov and Pushenko, 1996; Grunert et al., 2000; Komatsu et al., 2001; Krivonogov et al., 2014; Yu et al., 2017; Lehmkuhl et al., 2018; Rudaya et al., 2020; Mischke et al., 2020; Shao et al., 2022). Many of these lakes are essential elements of regional ecological and hydrological systems; the Aral Sea is a prime example of such interaction (Mischke et al., 2020).

Lake Chany is the largest endorheic lake in Siberia. It occupies the lowest point of the Baraba lowland in the south of West-Siberian Plain (Fig. 1). The lake has linear dimensions of about 90x90 km, and is rather complicated in shape; its spatial characteristics are shown in Table 1. The lake can be classified as shallow with an average depth of 2 m. The lake area has ranged from 1.7 to 2.2 thousand km^2 in recent decades (Vasiliev and Veen, 2015). The lake basin is complex and consists of several sub-basins and individual channel-linked lakes considering as the Chany lake system. The Kazantsev-Tagan, Chinyakhin and Yarkov sub-basins form the modern Lake Chany. The Yudin sub-basin was artificially separated by a dam in 1971 (Fig. 1C) and dried out (Vasiliev and Veen, 2015). The Malye Chany (Small Chany) is a separate lake connected with Chany Lake by a six km long channel. It receives water from Chulym and Kargat rivers that feed the Chany lake system and transfers water further to the main Lake Chany basin. This pattern of water supply causes a salinity gradient between parts of the lake system and therefore environmental and ecological differences. Thus, water supply from inflowing rivers is an important part of the Lake Chany total water budget (45 %, Savkin et al., 2006) and any hydrological change has a significant impact on the whole Chany lake system. Natural and anthropogenic fluctuations in water supply are crucial, as the lake is an important resource for agriculture and industrial fisheries, and events such as the drying-up in the early 1970s (Smirnova and Shnitnikov, 1982) and flooding in 2020–2021, caused significant public outcries.

Lake Chany has been a subject of intensive scientific investigation, and its modern environment, biology, biochemistry, ecology (e.g. Smirnova and Shnitnikov, 1982; Ioganzen and Krivoschekov, 1986; Ermolaev and Vizer, 2010; Vasiliev and Veen, 2015 and references therein) as well as modern water balance (Savkin et al., 2006, 2015) are well studied. The geological history of the lake is less well known. Early explorers and cartographers left evidence of a huge (fivefold larger than today) Chany lake system, as shown on old maps of the end of XVIII century (Savkin et al., 2015 and references therein); many historical data were summarized by Shnitnikov (1950, 1976). The data and 120 years long hydrological record suggest centennial-scale maxima in the second half of XVIII century and in the early XX century; the last one reached 2 m above the mean level measured in the XX century. The modern decadal-scale fluctuations are ± 1 m (Savkin et al., 2015). Shnitnikov (1950) considered these data in the frame of his Milankovitch theory-based conception of centennial-to-millennial fluctuations of the continental moisture supply and mountain glaciation cyclicity; this allowed him to construct a model of the Lake Chany level changes spanning last three thousand years.

The older history of Lake Chany is based on limited geological data. Morphology of the lake shores suggests up to 2 m higher past levels of the lake (Smirnova and Shnitnikov, 1982; Orlova, 1990). The shore bar and off-bar marsh series of Lake Malye Chany are dated from ca. 5.5 to 0.8 ^{14}C ka BP (Orlova, 1990). Until present, the only lake sediment core was obtained from the central part of the Yarkov sub-basin during its geological survey in 1980 (Smirnova and Shnitnikov, 1982). However, due to improper storage, the core dried and shrank from 5.0 to 3.5 m before palynological investigation and dating were performed. The only radiocarbon date of 3500 ± 80 a (TA-1390) was obtained for the 1.3–1.5 m interval of the core, and the age of the sediments was calculated on the basis of an assumed constant sedimentation rate resulting in a ^{14}C sediment age of 8.8 ka BP at the bottom of the core. The pollen analysis of this core revealed intervals with and without grains of aquatic plants. All these data are summarized in Tarasov and Pushenko, 1996. This study suggested that Lake Chany existed for a long time, at least since the Late Glacial (14 ka BP), and experienced a number of lake-level fluctuations. The level was normally high in the early and intermediate stages and lower in the later stages of the lake development.

Our study of the Chany lake system started in 2002. We drilled the Yarkov and Yudin sub-basins of Lake Chany and the Malye Chany Lake. Dating and biochemical, paleontological, and mineralogical investigations of the obtained cores (Krivonogov and Leonova, 2013, 2015a,b; Song et al., 2015; Song, 2016; Khazin et al., 2016; Zhdanova et al., 2017; 2019; Zhilich, 2015, 2019; Zhilich et al., 2015a,b, 2016) point to a different reconstruction from the previous studies of the history of the Chany lake system. These results suggest that the sediments in the lake basin are no older than 10 cal ka BP; Lake Chany as a large water body similar to the modern one appeared only at about 2 cal ka BP. In addition, the lake water supply was hampered by a specific structure of the catchment, which rivers included chains of intermediate lakes that collected river water and reduced the water transit to Lake Chany till ca. 2 cal ka BP (Krivonogov et al., 2018).

Despite the progress achieved, many issues in the Lake Chany history are still not clear. Parts of the lake may have specific development histories, and their sediment records should reflect these variations. Interdisciplinary research was needed to identify these differences and reconstruct the Lake Chany basin history in detail. This paper brings together all the data we obtained from multiproxy investigation of the Yarkov sub-basin of Lake Chany in order to disclose the history of this large endorheic lake and its relation with the environmental and climatic history of the South Siberian region. Many of the results from the Yarkov core were obtained as case studies for various projects and published in local journals or as conference abstracts, and used in theses; the objective of this paper is to bring these disparate findings (some of which are hard to obtain) together in a synthesis of the latest understanding of the Chany system.

2. Geography

The main geographic facts about Lake Chany and its catchment are summarized in Table 1. The Chany Lake catchment occupies an extensive area of flat topography in the central part of the Ob – Irtysh rivers interfluve, comprising sedimentary ridges and valleys oriented and tilted in a southwest direction. Topographic maps show the Chany Lake modern shoreline at the altitude of 106 m above the sea level. The lake occupies a closed depression formed in the center of a field of wind-blown SW-NE linear dunes (local name *griva*) of late-glacial age (Volkov, 1971). The dunes cross the basin and form linear islands and peninsulas in the lake (Fig. 1C). Ridge-and-hollow topography probably features the lake bottom that should result in uneven thickness of the lake sediments. The Yarkov sub-basin is circular in shape, unlike other sub-basins of Chany Lake (Fig. 1C). This shape is a result of the former wave erosion of the eastern and north-eastern banks of the Yarkov sub-basin by the prevailing SW winds during its high level periods, which is marked by a prominent wave-cut scarp located at a variable distance of tenth to hundreds meters from the lake's

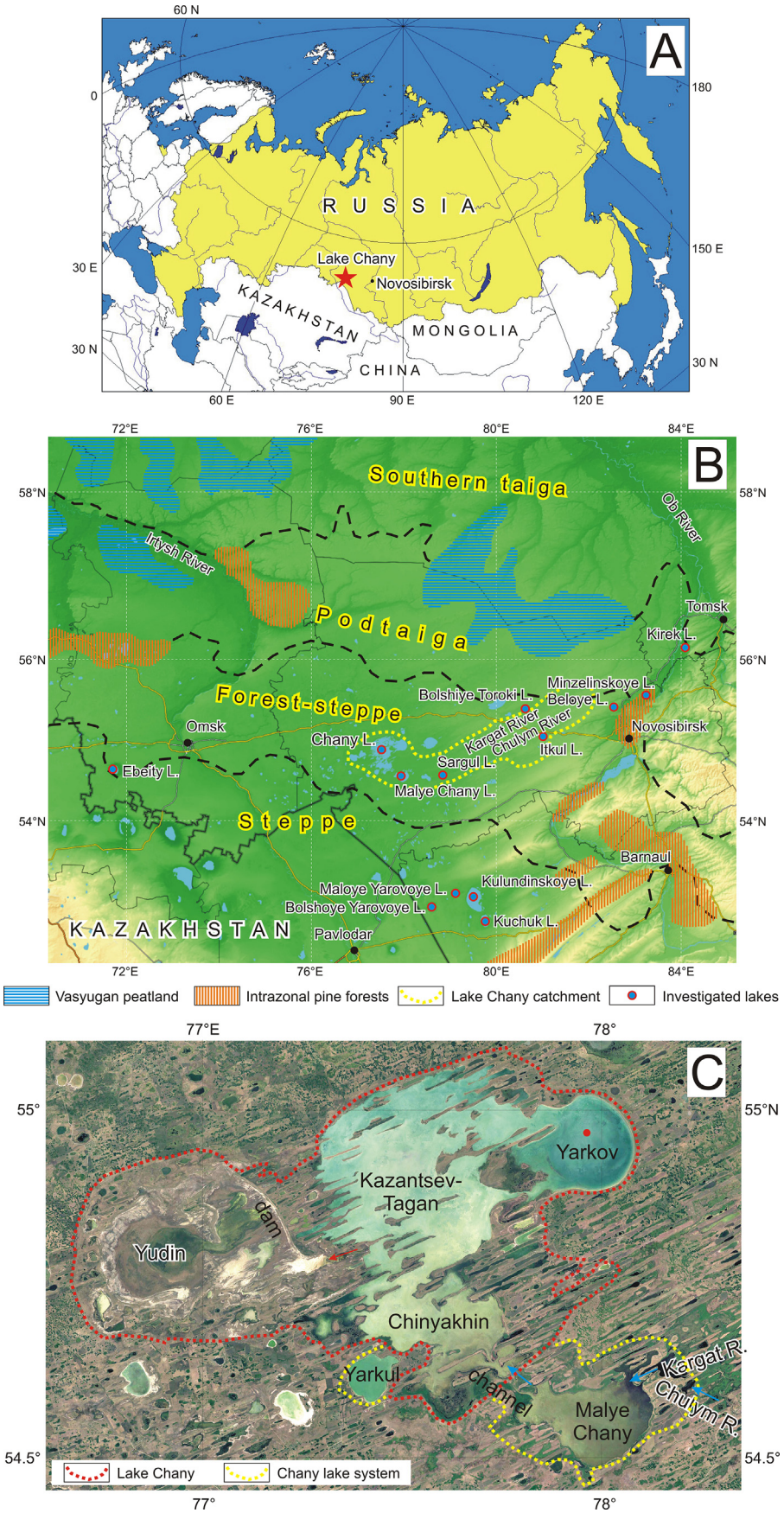

Fig. 1. Location. (A) General map. (B) Topography-based map of the region of investigation (Omsk, Novosibirsk and south of Tomsk regions), vegetation zones, and Lake Chany and other lakes discussed in paper. (C) GoogleEarth-based satellite image of Lake Chany and the Chany lake system; Red dot indicates the Yarkov sub-basin drilling locality. (For interpretation of the references to color in this figure legend, the reader is referred to the web version of this article.)

Table 1
Key facts on Lake Chany.

Parameter	Value
Max. length	91 km
Max. width	88 km
Long-term average area	2000 km^2
Max. depth	5.6 m
Average depth	2 m
Long-term average volume	4 km^3
Mineralization (Yarkov sub-basin)	6.6–8.0 g/dm^3

Data from Vasiliev and Veen (2015).

modern shore, dependent of topography. The water depth reaches 6 m with 3.1 m on average. The bottom relief in the middle of the Yarkov sub-basin is more or less flat, but varies within one meter (Savkin et al., 2015). Additionally, Yarkov is the deepest sub-basin, resulting in relatively low impact of waves on the bottom sediments.

Lake Chany is mainly fed by atmospheric precipitation to its surface and a narrow catchment around the lake, as well as by river runoff. The Chulym and Kargat rivers, which originate in the humid southern Vasyugan peatland region, flow southwest according to the general topography, enter Lake Malye Chany and feed all of Lake Chany. The river input in the lake's total water balance is 44 %—47 % and the input of atmospheric precipitation is 53 %—56 % (Savkin et al., 2006). The flow of river water forms a salinity gradient between the freshest Lake Malye Chany and the most saline Yarkov sub-basin; their mean values of total dissolved solids (TDS) are 1.2 and 7.1 g/dm^3, respectively, as measured in the summer months 1976–1978 (Savkin et al., 2015).

The climate in the region (Selegei, 2015) is temperate continental, characterized by Westerlies air masses and interior-continental position. The mean annual air temperature is about zero (+19 ℃ in July and −19 ℃ in January); the warm period in terms of mean monthly temperatures is seven months and in terms of solar radiation balance is eight months per year. Continentality leads to abrupt fluctuations and high temperature ranges during a year; the recorded absolute values are + 38 ℃ in July and −48 ℃ in January. The mean annual precipitation is 300–450 mm/yr. with maximum in the summer months. The potential evaporation is 400–550 mm/yr. The arid territories of Kazakhstan, located in the south-west along the Atlantic air mass route, reduce humidity of the Chany region.

Soils of the region reflect the climatic features, local topography, and groundwater regime (Kazantsev et al., 2015) and vary from chernozem on drier and higher landscapes to solonchak (salic soil) in wet depressions. Salinization is a major factor of soil quality near Chany Lake. Wet landscapes near less saline lakes and rivers have meadow-swamp and swamp soils with variable amounts of peat accumulation.

The forest-steppe vegetation around Lake Chany is a mosaic of forest groves, steppes, meadows, solonchak meadows (in wet depressions with saline soils), and water meadows (Korolyuk et al., 2015). The share of forest in the landscape decreases from north-east to south-west. Birch, *Betula pendula* Roth and *B. pubescens* Ehrh., and aspen, *Populus tremula* L., are dominant trees. Large forest massifs mostly occupy higher and drier areas. Small groves, locally known as "kolki" (plural) or "kolok" (single), occupy flat depressions which are wet in their central parts and overgrown by willow (*Salix cinerea* L., *S. gmelinii* Pall., *S. pentandra* L. and *S. rosmarinifolia* L.). Meadows and steppe meadows are widespread in the region. The dominant grasses are *Calamagrostis epigeios* (L.) Roth, *Poa angustifolia* L., *Phleum phleoides* (L.) H. Karst., *Elytrigia repens* (L.) Nevski, and *Bromopsis inermis* (Leyss.) Holub. Solonchak meadows scattered in salinized depressions and around saline lakes are dominated by *Alopecurus arundinaceus* Poir., *Hordeum brevisubulatum* (Trin.) Link, *Carex aspratilis* Wahlenb., *Artemisia nitrosa* Web. ex Stechm., *Puccinellia tenuissima* Litv. ex Krecz., and such succulent halophytes as *Salicornia perennans* Willd. and *Suaeda corniculata* (C.A. Mey.) Bunge. Water meadows occupy shallow-water depressions overgrown with *Phragmites australis* (Cav.) Trin. ex Steud. The aquatic and lakeshore communities of the lakes are highly dependent on their salinity and depth. In the Lake Chany system, aquatic and submerged vegetation includes 26 species of vascular plants and charophytes; *Phragmites australis* and several species of *Potamogeton* are dominant. The Yarkov sub-basin, with its high depth and intensive near-shore wave-cut activity, is unfavorable for higher water vegetation.

Other lacustrine biota (Kirillov et al., 2015) involved in sediment formation is phytoplankton, zooplankton and zoobenthos. Phytoplankton includes 158 species, with green algae predominating (40 %—50 %); its biodiversity decreases significantly with increasing water salinity. Zooplankton, 65 species, are mostly non-carnivorous and include Rotatoria (29), Cladocera (27), and Copepoda (9). Macrozoobenthos (>130 species) comprise Chironomidae (45 species), Mollusca (29 species) and Hexapoda (15 species). There is no data on modern ostracods of the Chany lake system, though they are known from Holocene record (Khazin et al., 2016).

The biomass of the lake is mainly controlled by water mineralization and to a lesser extent by changes in the water level/volume of the lake (Kirillov et al., 2015). For example, Ermolaev (1998) reported 168 mg/dm^3 of phytoplankton biomass in Lake Malye Chany (salinity 0.88 g/L) and only 2.43 mg/dm^3 in the Yarkov sub-basin (salinity 7.1 g/L). In contrast, the total biomass of zooplankton is 5.53 g/m^3 in Lake Malye Chany and 20.926 g/m^3 in the Yarkov sub-basin (Kirillov et al., 2015). As for the benthos of the Yarkov sub-basin, the main clayey part of its bottom has no zoobenthos, while it is rich in the near-shore sandy part (17 g/m^2), where *Chironomus* larvae dominate.

3. Materials and methods

The Yarkov sub-basin of Lake Chany was drilled by our team in the spring 2008 from the ice near its central part: coordinates N 54.9624 E 77.9595, depth 5.6 m from the ice surface (Fig. 1C). Four sediment cores (Yarkov 2008 01 – 04) were derived from the same location several meters apart. The cores were retrieved by a 2-m long and 5.5 cm diameter Livingstone-type sampler with a plastic liner inside; the diameter of the cores was 4.6 cm. A gentle vibration technique allowed us to penetrate the entire lake sediment sequence and enter the basal sediments of non-lacustrine origin. Since the lake sediments are soft and highly water-saturated, they are subjected to uneven compression during drilling operations, resulting in shifting of visible sediment layers; however, the sediment stratigraphy allowed us to correlate the cores (see section 4.2 and Supplementary Data, Table S1).

The longest and possibly most complete cores 02 and 04 were opened in the lab, described, photographed and subsampled for the following analytical methods: the 325-cm long Yarkov-02 core for radiocarbon and ^{210}Pb dating, sedimentology, mineralogy, geochemistry (23 chemical elements), and isotope (^{18}O and ^{13}C in carbonates) and biomarker (*n*-alkanes and long chain alkenones) analyses; the 320-cm long Yarkov-04 core for pollen, diatom and chironomid analyses. Separately, the 276-cm long Yarkov-03 core was used for rock magnetic studies. The results of the analyses were used to detect signals of lake ecosystem and climatic changes. In addition, the following vegetational and climatic reconstructions were derived from the data: pollen-based vegetation types by the biomisation method, and pollen-based (mean annual

precipitation) and chironomid-based (mean July temperature) by transfer function approach with regional calibration datasets. A detailed description of the methods is in Supplementary Data Text 1 and a summary is provided at the beginning of each subsection of section 4.

4. Proxies from the Yarkov sediment cores

4.1. Chronology

AMS radiocarbon dating of the whole Yarkov-02 core was done at KIGAM, Korea, Beta Analytic, USA, and Novosibirsk, Russia. The dates were calibrated in CALIB 8.2 WWW program and converted into before present (BP) timescale units; the ages used in the paper are rounded to kiloyears (ka BP). The age of the upper 14 cm of the sediment has been further assessed by the ^{210}Pb method at the Institute of geology and mineralogy SB RAS, Novosibirsk, Russia; the age units are years before 2008, which is the coring year. See Supplementary Data Text 1 for details.

In total, 14 radiocarbon dates are available (Table 2). Four dates obtained from total inorganic matter (TIC) and carbonates of ostracod shells gave considerably older ages reflecting contamination of the sediments by old carbonates abundant in the surrounding loess-like sediments. We omitted those dates from the age model. Eleven dates obtained from total organic matter (TOC) are stratigraphically consistent and were used for the age model (Fig. 2A). A third-order polynomial trend describes the dataset with $R^2 = 0.9956$. The trend line shows significant variations in sedimentation rate along the core. The variations are visually consistent with the general stratigraphy (see section 4.2), allowing a piecewise linear approximation for the core intervals (Fig. 2A). The trends obtained and the corresponding sedimentation rates are shown in Table 3.

We analyzed the robustness/applicability of the two age models, third-order spline and piecewise linear trends, by original calibrated radiocarbon dates and corresponding age values from the trends (Supplementary Data Table S2). The values show a slight discrepancy at the top of the data set, which increases significantly at the bottom. The effect is a result of the shape of the trend graphs: their lower, shallow slopes yield larger differences (Fig. 2A). As the piecewise linear approximation gives smaller differences than the polynomial, we prefer it as the age model for Yarkov-02. The values predicted by this model and the radiocarbon dates are essentially 110 years apart; only one record at a depth of 140 cm shows an exceptionally high difference and should be omitted (Supplementary Data Table S2). We conclude that the model allows us to use a hundred year resolution in possible reconstructions.

According to the model, the age of the surface of the core is 346 yrs. BP. We consider this value as an old carbon effect of the sedimentary basin and subtract it from the model predicted ages used in the paper. Thus, the extrapolated "true" age estimate of the bottom of the lake-basin sediments at a depth of 274 cm is 9.1 ka BP; the boundary of 200 cm between the upper grey and lower blackish lake sediments is at 3.6 ka BP.

The ^{210}Pb concentrations data provided additional information on age (Zhdanova et al., 2017). The calculations based on the constant rate of supply model suggest 87 ± 17 years age for the sample at 12–14 cm and a sedimentation rate of 0.2 to 0.13 cm/yr. for the 0–13 cm interval (Fig. 2B). The radiocarbon-based age model extrapolates 72.5 years at 13 cm depth and a sedimentation rate of 0.18 cm/yr. Despite the similarities in sedimentation rates, the dates converted to AD correspond to 1925 and 1878, respectively, with a difference of 47 years. The CE 1950 level is at 11 and 5 cm, respectively.

4.2. Stratigraphy

The following description refers to the Yarkov-02 core selected as the reference (Fig. 3):

Grayish **Layer 1 (0–200 cm, 0–3.6 ka BP)** includes **Sub-layer 1a (0–140 cm, 0–1.5 ka BP)** – waterlogged silt with uncommon visible decayed organics and **Sub-layer 1b (140–200 cm, 1.5–3.6 ka BP)** – sandy silt with ostracod and rare gastropod shells in its lower part.

Blackish **Layer 2 (200–274 cm, 3.6–9.1 ka BP)** includes **Sub-layer 2a (200–250 cm, 3.6–7.3 ka BP)** – sandy silt with high organic content and visible plant remains and **Sub-layer 2b (250–274 cm, 7.3–9.1 ka BP)** – less sandy silt.

Layer 3 (274–325 cm) – much denser brownish-gray sandy silt.

Layer 3 is material underlying the lake basin, a loess-like eolian loam of Late Pleistocene age, which is widely distributed in the region and covers the surrounds of the lake. Layers 1 and 2 formed in the lake basin. Since only the Yarkov-02 core was dated, a stratigraphic correlation was made between it and cores 03 and 04 (Supplementary Data Table S1). This allowed us to match the sampling schemes of the cores and to use a timescale to integrate the results.

Table 2
Radiocarbon dates and calendar ages of Yarkov-02 core sediments.

Depth (cm)	Lab ID	^{14}C date, yrs BP	δ^{13}C	Material	Calendar age	
					Interval (yrs)	Median probability
8	Beta 393,422	290 ± 30	−27,9	TOC	158–452	385
33*	KIGAM ISa120003	520 ± 30	−31,9	TOC	506–623	535
74	Beta 393,423	870 ± 30	−27	TOC	689–902	765
105*	KIGAM ISa120004	1010 ± 30	−22,2	TOC	798–958	925
120	Beta 422,332	1510 ± 30	−27.5	TOC	1310–1510	1380
127	GV**	5134 ± 246		TIC		***
140	Beta 422,333	1690 ± 30	−26.3	TOC	1528–1695	1580
150	Beta 393,424	2260 ± 30	−26,9	TOC	2155–2343	2231
190	Beta 393,425	3090 ± 30	−22,8	TOC	3219–3373	3295
191*	KIGAM ISa120005	6040 ± 50		Carbon from ostracod shells		***
193	GV**	4568 ± 242		TIC		***
202	Beta 393,426	3630 ± 30	−23,9	TOC	3845–4078	3942
223*	KIGAM ISa120006	4960 ± 40	−25,3	TOC	5593–5857	5679
252	Beta 422,334	6890 ± 30	−24.1	TOC	7665–7823	7718
261	GV**	9973 ± 358		TIC		***

* Courtesy of Dr. Kim Ju Yong, Korean Institute of Geosciences and Mineral Resources (KIGAM), joint research.
** GV is the lab code of the Novosibirsk AMS Facility; the dates have been obtained in a testing period and have no lab numbers.
*** Rejected because of stratigraphical inconsistency.

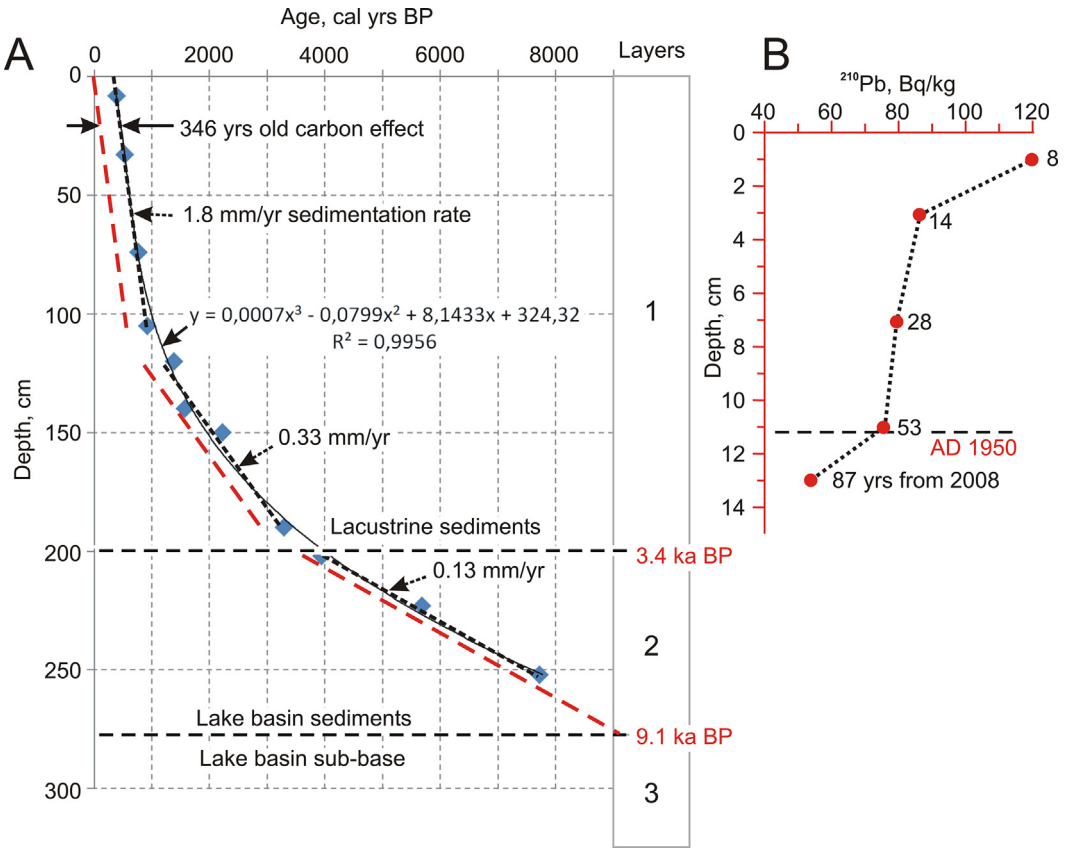

Fig. 2. (A)Age model based on radiocarbon dates for the Yarkov-02 core. Red dashed lines show piecewise linear approximation of probable ages with an old carbon effect equal to 346 years. B: Age model calculated from ^{210}Pb concentrations in the upper part of the Yarkov-02 core. Adapted from Zhdanova et al. (2017). (For interpretation of the references to color in this figure legend, the reader is referred to the web version of this article.)

Table 3
Linear trends applied for the Yarkov-02 core, average sediment rates, and sediment input.

Interval (cm)	Trend line		Sedimentation rate		Average water saturation (%)	*Average specific weight of mineral part (g/cm^3)	Weight of mineral part in sediment (g/cm^3)	Sediment input (g/cm^2 * yr^{-1})
	Equation	Validity value (R^2)	(yrs/cm)	(cm/yr)				
0–105	$y = 5.5672x + 346.31$	0.9992	5.6	0.18	64.4	2.65	0.94	0.169
120–190	$y = 30.376x - 2366.4$	0.9772	30.4	0.033	40.1	2.63	1.58	0.052
202–274	$y = 75.186x - 11,185$	0.9977	75.2	0.013	28.6	2.63	1.88	0.024

* Specific weight of mixture of quartz, plagioclase, and carbonates in proportions inferred from mineralogical data (Section 4.2).

4.3. Sedimentological data

The proportions of the main sediment components: authigenic, terrigenic and biogenic, were estimated from 5 cm^3 samples taken by a syringe with every 5 cm interval of the Yarkov-02 core; the terrigenic component was analyzed with a laser particle-sizer. See Supplementary Data Text 1 for details.

Sedimentological analysis confirms the visually estimated layers and their boundaries (Fig. 3). The moisture content of the sediments gradually increases from bottom to top and is consistent with the decrease in density; the sandy part of the core is denser. The proportions of the major sediment components show fairly consistent trends along the core. The organic matter is about 10 dry wt.% in the lower half and gradually increases to 20 % in Sublayer 1a. The authigenic, predominantly precipitated carbonates, and terrigenic components change significantly and show a negative correlation: authigenic increases and terrigenic decreases upwards. The values fluctuate near 20 % and 65 %, respectively, in Layers 3 and 2 and generally converge to about 40 % from the bottom to the top of Layer 1. Minor fluctuations in all three graphs may indicate short-term changes in the lake sedimentation, which, however, is unlikely to be reliably decoded.

The laser grain size analysis shows the predominance of silt to fine sand fractions in the core (Fig. 4). Unimodal distribution with coarse silt peak is typical for Sub-layer 1a; sublayer 1b is considerably sandier. Layer 2 shows variable grain sizes from aleurite to psammi-aleurite, and its lowest part resembles bimodal histograms from the loess-like sediments, which are sandy silts.

Reconstruction of the sedimentation environment of the lake.

Thus, the sediment structure and its composition imply variable sedimentation conditions along the core. It is probably that the blackish sandy silts of Layer 2 formed in a wet "swamp-and-soil" environment, which is confirmed below by other analytical methods. The grey-colored Layer 1 obviously formed in the lake, which was shallower in the lower part and deeper above. We conclude that the increase in the lake-derived organic and authigenic components reflects the eutrophication and salinization of the lake, while the transport of the terrigenic mineral component to the lake

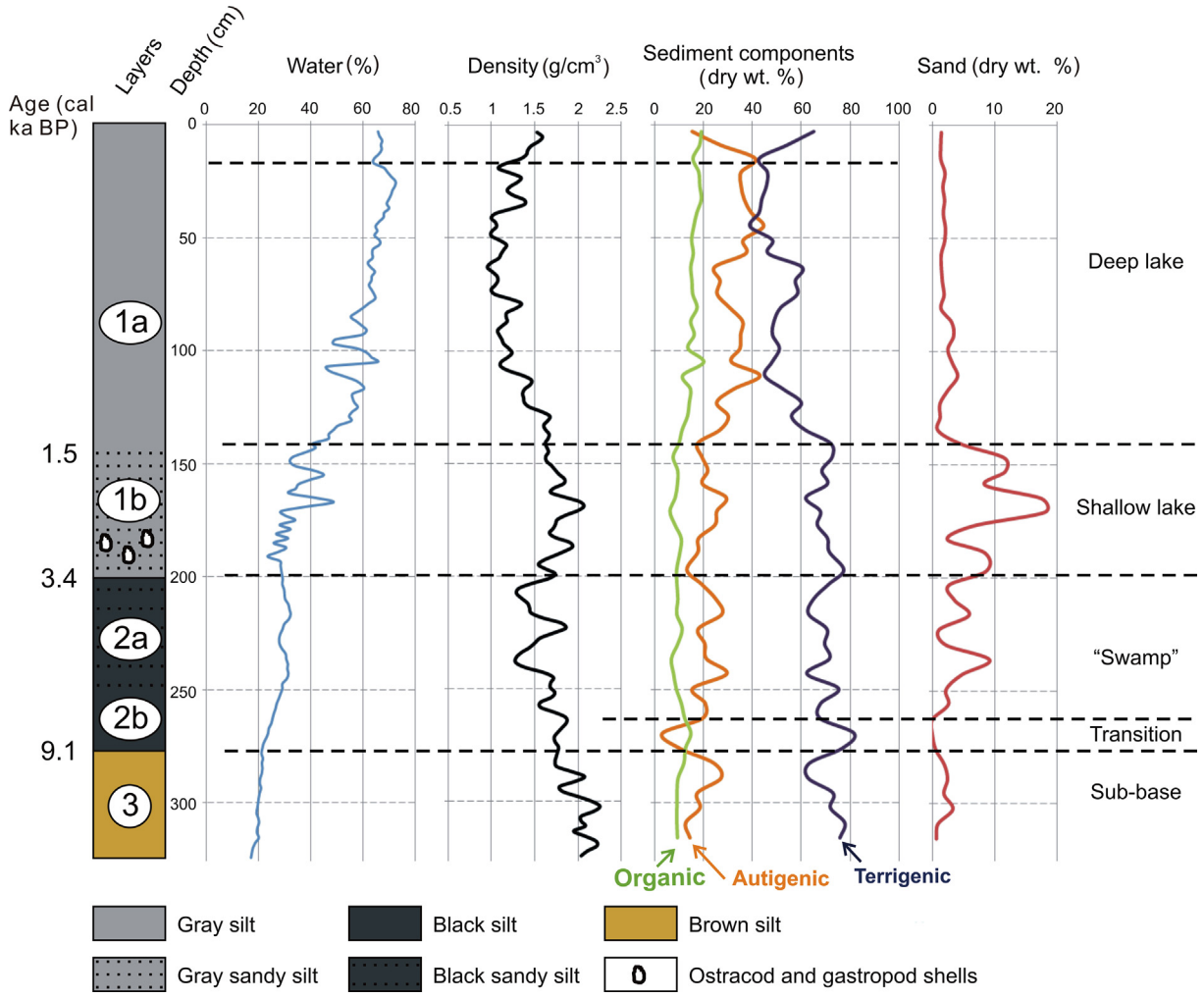

Fig. 3. Stratigraphy and proportions of main sediment components in Yarkov-02 core.

was more-or-less constant during Layer 1 accumulation. Oddly, the inversion of the parameters in the upper 20 cm of the core suggests desalinization, which is inconsistent with the shallowing of the Chany lake system in recent centuries (Savkin et al., 2015). We explain atypically increased density and lowered water saturation of the sediments in this interval by the reduction of the water content at the top of the core during its retrieval and storage.

In addition, the age model (section 4.1. Chronology) indicates a considerable difference in the sedimentation rates and sediment input between the layers and sub-layers (Fig. 2A, Table 3). The calculated average sedimentation rates in cm/yr differ by a factor of 5.5 between 0 and 105 and 105–190 cm intervals (Sub-layer 1a and Sub-layer 1b, respectively), and by a factor 14 between 0 and 105 and 202–274 cm intervals (Sub-layer 1a and Layer 2, respectively). The sediment input in $g/cm^2 * yr^{-1}$ differs by a factor 3 and 7, respectively.

4.4. Mineralogical data

The mineral composition of the Yarkov-02 core was investigated by X-ray diffractometry and infra-red spectroscopy at the Institute of Geology and Mineralogy SB RAS, Novosibirsk. See Supplementary Data Text 1 for details.

There is a predominance of quartz, feldspars (mainly plagioclase) and carbonates in the sediments; mica, chlorite and pyrite are subordinate (Fig. 5, percentages were calculated from the total mineral component taken as 100 %). Most of the minerals are terrigenic, but carbonates and pyrite are authigenic. Carbonates are relatively high in the loess-like substrate (310–274 cm) and extremely high, up to 30 %, in the base of the lake basin sediments (274–245 cm). Above, the share of carbonates increases from almost zero to about 25 %, and from a depth of 130 cm varies between 15 % and 28 %.

The XRD profiles of the sediments revealed variations in the minerals of calcite-dolomite series (low-Mg, intermediate-Mg, and high-Mg calcite) and aragonite. Low-Mg calcite is dominant in the spectra and extremely prevalent in the lower part of the core, 310–200 cm. Above this level, the proportions of other Ca minerals reflect the likely changes in the lake environment reconstructed with the addition of $\delta^{13}C$ and $\delta^{18}O$ data (Fig. 5). The stable isotope ratios in the Ca-minerals are negative throughout the core.

Our updated interpretation of the mineralogical data infers two mineralogical zones (MZ) and five sub-zones (MSZ) within the lake-basin and lacustrine parts of the Yarkov-02 core (Layers 2 and 1).

MZ I (274–200 cm, 9.1–3.6 ka BP) is indicated by predominant precipitation of low-Mg calcite and low stable isotope ratios.

MSZ Ia (274–245 cm, 9.1–6.9 ka BP) shows the peak of carbonates probably leached from the carbonate-rich Layer 3 at the beginning of the wetting of the lake basin (Sub-layer 2b).

MSZ Ib (245–200 cm, 6.9–3.6 ka BP), in turn, shows the carbonate minimum and represents low-saline environment (Sub-layer 2a).

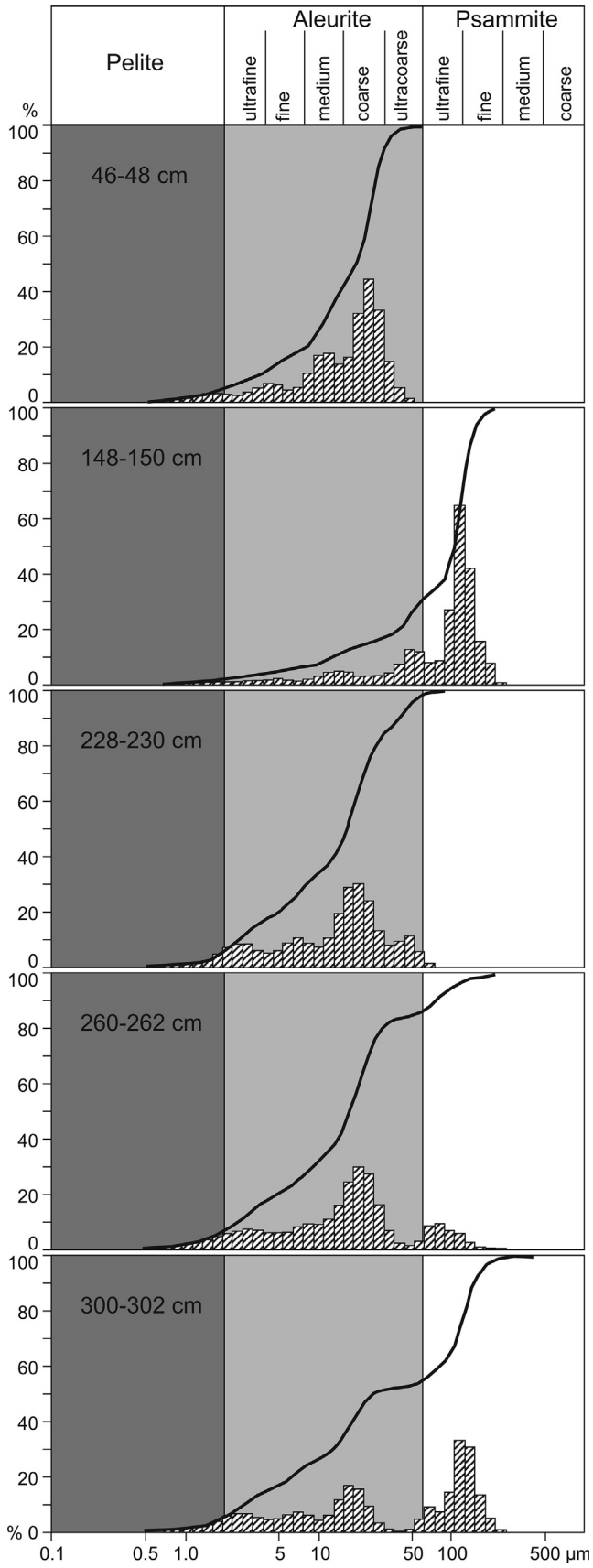

Fig. 4. Typical grain size histograms for main sub-layers of Yarkov-02 core.

MZ II (200–0 cm, 3.6–0 ka BP) represents a "geochemically matured" saline lake with precipitation of various minerals of the calcite-dolomite series.

MSZ IIa (200–130 cm, 3.6–1.2 ka BP) shows a gradual increase in the total carbonates and the active precipitation of high-Mg calcite and excess-Ca dolomite (Sub-layer 1b) and a synchronous increase of $\delta^{18}O$ and $\delta^{13}C$.

Sub-zones IIb and IIc have maximum concentration of carbonates with high parts of low-Mg and intermediate-Mg calcite.

MSZ IIb (130–50 cm, 1.2–0.3 ka BP) is clearly demarcated by the peak of aragonite.

MSZ IIc (50–0 cm, 0.3–0 ka BP) is typical for low-Mg and intermediate-Mg calcite, while the top 20 cm of the sediments show decrease in the latter replaced by high-Mg calcite and excess-Ca dolomite.

4.5. Geochemical data

The element composition of the sediments of the Yarkov-02 core was determined by synchrotron radiation X-ray fluorescence analysis at the Institute of Nuclear Physics, Novosibirsk, and atomic-absorption spectroscopy at the Earth Crust Institute SB RAS, Irkutsk. See Supplementary Data Text 1 for details.

Fig. 6 shows the distribution of normalized concentrations of 20 chemical elements. Three of them, Ca, Sr, and Br, show clear increases along the core while other elements show slightly decreasing or only slightly varying concentrations. The concentrations of most elements vary according to the stratigraphy. The upper part of the figure shows elements indicating significant geochemical changes at the boundaries of Layers 1 and 2, and their sub-layers. Calcium values are average in Layer 3, increase sharply in Sub-layer 2b, then show a large decrease in Sub-layer 2a. They increase steadily in Sub-layer 1b, then remain high in Sub-layer 1a. Strontium changes in similar way, which can be explained by the Ca/Sr isomorphic effect. Other elements placed at the top of the figure, unlike Ca and Sr, show an increase in Sub-layer 2a, which is the "response" to the decrease of Ca and Sr, and likely just reflects changes in the proportional representation of the constituent elements. Y, As, Zr, Ge and U, in the lower part of the figure, show an increase for the whole interval of the sand-rich sub-layers 2a and 1b. Some paired elements, Cu and Zn and Mn and Br, have sharp peaks; for the latter pair the peaks match the boundary between Layers 1 and 2.

Reconstruction of the geochemical environment of the lake.

Geochemical and mineralogical data thus clearly indicate predominant deposition but also variation of calcium carbonate in the lake. The fluctuations in all proxies are closely correlated with the sediment stratigraphy. The stable-isotope ratios in the Ca-minerals (Fig. 5) are negative throughout the core, suggesting the depletion of heavy isotopes, likely controlled by the share of meteoric waters in the lake basin water budget (Veizer, 1983; Talbot, 1990; Last and Ginn, 2005); the influence of other fractionation factors on the composition of the isotopes in the region is uncertain. In general, the ratios in the lake-basin sediments are lower below and higher above the 200 cm boundary compared to those of the underlying loess. **MZ I**, Layer 2, indicates predominant low-Mg calcite and suggests its precipitation from medium-carbonate waters of moderate salinity (Nechiporenko and Bondarenko, 1988); the isotopic composition infers the predominance of meteoric waters in the water budget. **MZ II**, Layer 1, shows a variable environment. The presence of excess-Ca dolomite in **MSZ IIa**, Sub-layer 1b, may indicate a playa environment (Last, 1990), however, the ostracod shells abundant in this layer do not

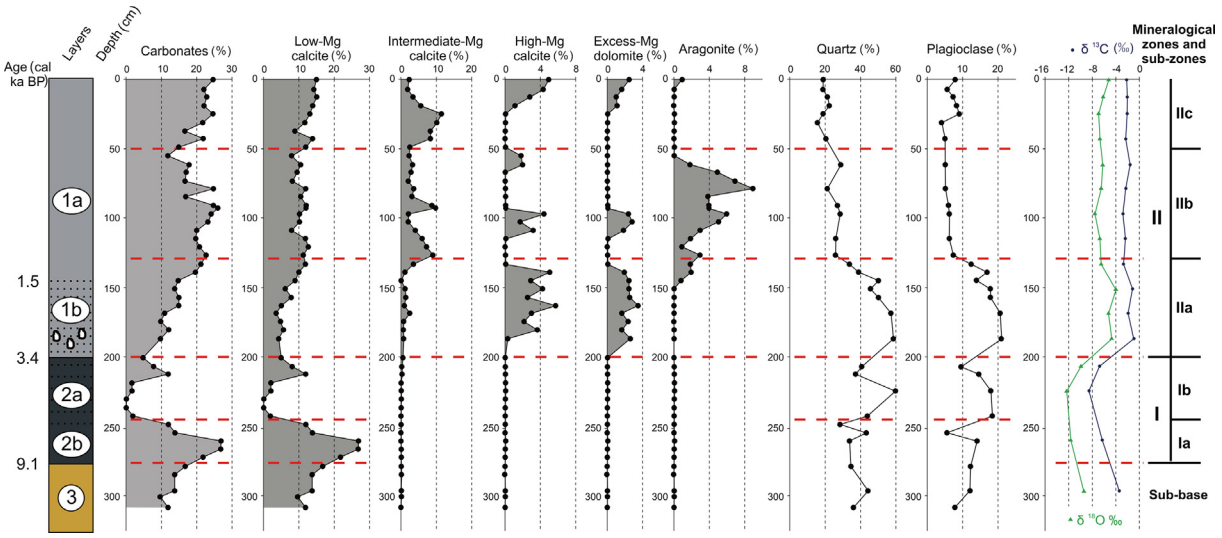

Fig. 5. Mineralogical data from Yarkov-02 core. Adapted from Zhdanova et al. (2017).

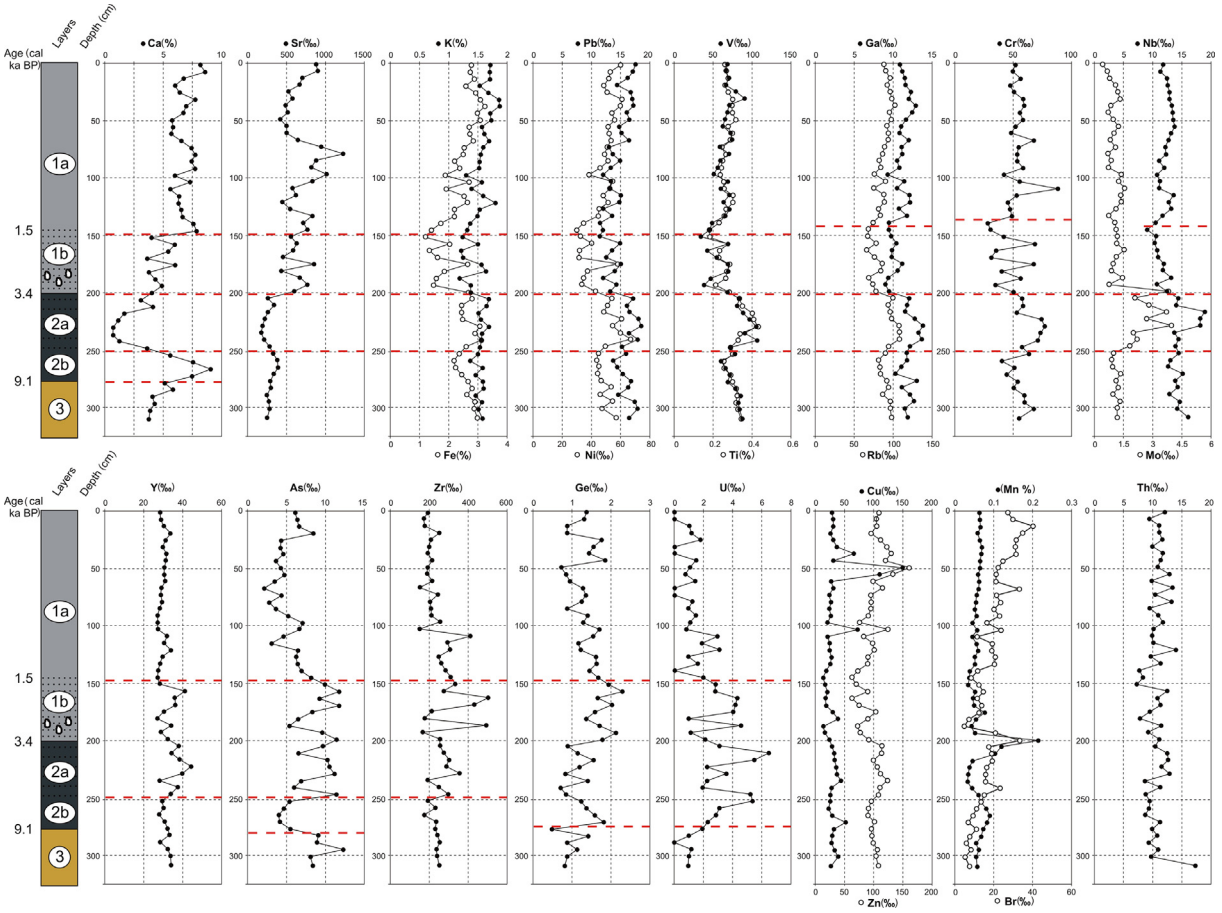

Fig. 6. Chemical elements contents data from Yarkov-02 core.

support the lake drying out. A large shallow lake is also supported by a synchronous increase of $\delta^{18}O$ (increased evaporation) and $\delta^{13}C$ (increased primary productivity of the lake and/or reduced atmospheric precipitation). Decreases in the curves indicate a larger water input, i.e., a deeper lake in the overlying sub-zones. **MSZ IIb**, most of Sub-layer 1a, is clearly demarcated by the peak of aragonite, which can be formed on calcite seeds at high concentration of Mg^{2+} ions in water (Leeder, 1982; Nechiporenko and Bondarenko, 1988). **MSZ IIc**, the top 20 cm of Sub-layer 1a, shows a decrease in aragonite, it being replaced by high-Mg calcite and excess-Ca dolomite, which may reflect the current shallowing of the Chany lake system.

4.6. Rock magnetic data

All rock magnetic measurements of the Yarkov-03 core were performed in the Laboratory of Geodynamics and Paleomagnetism of the Institute of Petrol Geology and Geophysics SB RAS, Novosibirsk, according to standard procedures (see Supplementary Data Text 1 for details). The data clearly divide the core into three zones (RMZ) (Fig. 7).

RMZ I (276–219 cm, 9.1–5.0 ka BP) covers most of Layer 2. Its concentration-dependent parameters χ_{fer}, M_{fer} and M_{rs} indicate a relatively high concentration of magnetic minerals (Fig. 7A). Low S values and increased B_{cr}/B_{cf} and χ_{fer}/M_{rs} ratios indicate the highest contribution of highly coercive minerals and the largest magnetic grain sizes over the core, respectively (Fig. 7C). Similarly, the scatter of all rock magnetic parameters is the smallest.

RMZ II (219–180 cm, 5.0–2.8 ka BP) has the maximum scatter of all parameters, the highest values of concentration-dependent parameters, high B_{cf} and S, and the lowest B_{cr}/B_{cf} ratios (Fig. 7A, B), indicative of highly variable sedimentation environment interpreted as a transition zone.

RMZ III (180–0 cm, 2.8–0 ka BP) covers Layer 1. Its concentration-dependent parameters show low amounts of magnetic minerals, 5–7 times less than in RMZ I, and the B_{cr}/B_{cf} values are also lower (Fig. 7A, B); the parameters have small scatter. S values are low near the bottom and the top of the zone and increase roughly to the level of RMZ I in the middle (Fig. 7A) indicating an increase in high coercivity minerals.

The paramagnetic content is nearly equal all across the core. A slight decrease of χ_p is observed between 180 and 120 cm (Fig. 7A).

The domain states of the magnetic grains in the zones are slightly different. The Day-Dunlop plot suggests a pseudo single domain (PSD) for most samples (Fig. 7C); only two samples are in multi-domain (MD) state. However, the samples from RMZ I are tightly grouped alongside the theoretical SD-MD mixing curve (Dunlop, 2002), which suggests up to 20 % of single-domain (SD) grains. The samples from RMZ III are stretched along the theoretical curve and indicate 10 % to 40 % of SD grains. RMZ II shows the greatest variation in the domain states: SD grain concentration changes from 5 % to 80 %, typically 40 %—80 %.

Unmixing of the M_{rs} curves reveals four components with maxima of coercive spectra at 2–30 mT, 35–40 mT, 45–65 mT and 200–500 mT. According to Egli (2004), these components correspond to detrital magnetite + extracellular magnetite (D-EX), pedogenic magnetite (PD), biogenic soft magnetite (BS) and high-coercivity hematite (H), respectively. Variations in the magnitudes of each unmixed component and their relative percentages (Fig. 7B) show considerable predominance of BS and subordinate content of D-EX and H over the core, with the exception at the 245–190 cm interval, where the D-EX component is missing and the PD component is present. The BS component is negatively correlated with D-EX and H, but there is no correlation between D-EX and H.

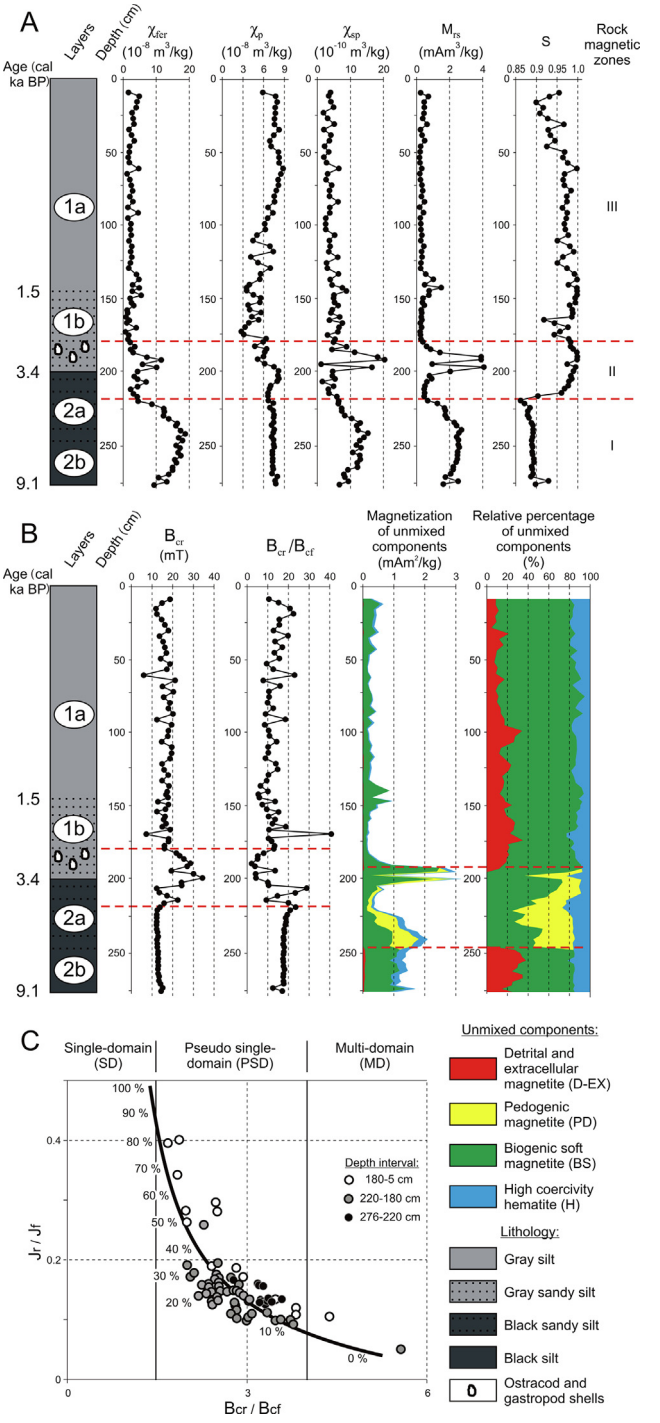

Fig. 7. Rock magnetic data from Yarkov-03 core. (A) Selected concentration-dependent parameters. (B) Selected structurally sensitive rock magnetic parameters and distribution of unmixed components. (C) Characteristics of the magnetic state of grains by hysteresis parameters on the Day–Dunlop theoretical diagram (Day et al., 1977; Dunlop, 2002).

4.7. Biomarker data

The composition and proportions of *n*-alkanes and long chain alkenones in the Yarkov-02 core were investigated using standard technologies of extraction with the following identification at Agilent 7890 Gas Chromatography facility with Flame Ionization Detection at the University of Hong Kong. See Supplementary Data Text 1 for details.

n-Alkane proxies.

The ACL (average chain length), Paq (percentage of aquatic plant input), and CPI (carbon number preference index) records (Fig. 8) share similar fluctuations corresponding to the core lithology; the main change occurred about 4 ka BP, which roughly corresponds to the boundary between Layers 1 and 2 at a depth of 200 cm (Fig. 3). The records show minor, gradual fluctuations in the bottom part but fluctuate rapidly in the top part. The ACL values range from 25.2 to 29.5 with an average of 28 (Fig. 8); the Paq ranges from 0.1 to 0.8 with an average of 0.4, and shows mirrored pattern with ACL. CPI ranges from 3.1 to 8.5, averages to 6.0, and fluctuates similarly to ACL, but the frequency of CPI changes at the top is higher.

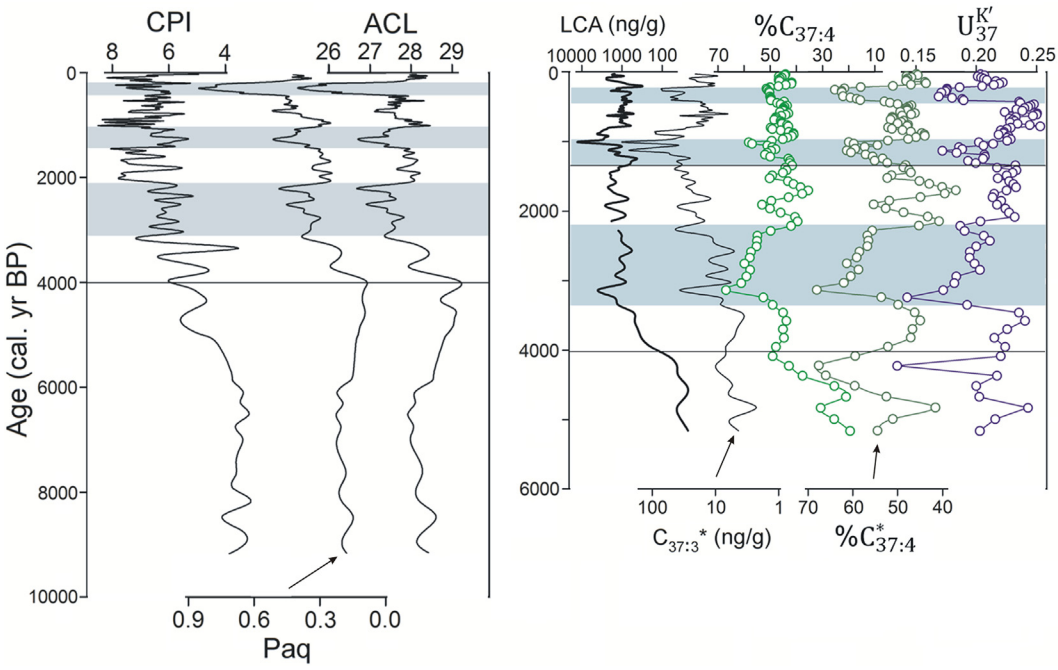

Fig. 8. Left panel: *N*-alkane ACL, Paq, and CPI proxies from Yarkov-02 core. Right panel: Long-chain alkenones proxies from Yarkov-02 core: total LCA, $C^{*}_{37:3}$, $C_{37:4}$, $C^{*}_{37:4}$, and $U^{K\prime}_{37}$. Colored bands indicate three episodes of colder and less saline-water environments.

The 4–0 ka BP interval includes three episodes with a significantly low ACL and CPI and a high Paq ca. 150–450 yrs. BP, 1.0–1.4, and 2.2–3.1 ka BP, marked with grey bands in Fig. 8. The second band overlaps the boundary of Sub-layers 1a and 1b dated at 1.5 ka BP.

LCA proxies.

The $U^{K\prime}_{37}$ values (see Supplementary Data Text 1), although with large fluctuations, range from 0.13 to 0.25 in the core with an average of 0.21 (Fig. 8). Three episodes (180–450 yr BP, 1.0–1.4, and 2.1–3.3 ka BP) with lower-than-average $U^{K\prime}_{37}$ values are easily recognizable in the younger than 4 ka part of the core. They largely coincide with the three above mentioned *n*-alkane record derived episodes with high Paq and low ACL and CPI.

The $\%C^{*}_{37:4}$ varies in a relatively narrow range from 37 to 68 % with an average value of 52 %, whereas the $\%C_{37:4}$ shows a rapid increase from 20 to 40 % in the older than 4 ka BP interval and stays mostly > 40 % in the younger one. Despite differences in trends, the $\%C^{*}_{37:4}$ and $\%C_{37:4}$ show similar detailed variations with higher-than-average values only in the three above-mentioned episodes.

The $C^{*}_{37:3}$ LCA and total LCA show similar trends and values, which gradually increase to 3.2 ka BP and then fluctuate around their mean values, but do not follow the variation of other indices perfectly. The total LCA varies from 45 to about 16,000 ng/g, with an average of 990 ng/g of dry sediment. The $C^{*}_{37:3}$ LCA content varies from 2 to 313 ng/g, on average 20 ng/g. Both parameters increase distinctly at 180–450 yrs. BP and 1.0–1.4 ka BP intervals. The episode 2.1–3.4 ka BP, although having low $U^{K\prime}_{37}$ values and high percentage of tetra-unsaturated LCAs, is not recognized.

Reconstructions from biomarker data.

Both *n*-alkane and LCA proxies similarly indicate the three above mentioned episodes. *n*-Alkanes suggest the prevalence of submerged and emerged aquatic macrophytes, algae, and bacteria during them and the $U^{K\prime}_{37}$ values of LCA suggest colder environments with a higher portion of lacustrine organic matter. Other intervals of the core with high $U^{K\prime}_{37}$, ACL and CPI and low Paq represent warmer environments and increased terrestrial input. The *n*-alkanes in the > 4 ka BP part of the core with the highest ACL and lowest Paq were also mainly contributed by terrestrial plants. The $\%C^{*}_{37:4}$ values of LCA may indicate more freshwater conditions, thus higher lake levels in these three episodes. The $C^{*}_{37:3}$ LCA and total LCA are also helpful to estimate the salinity variation indicating two of the above three cold and wet episodes as low saline. However, the episode of 2.1–3.4 ka BP is not recognized. This may result from low salinity insufficient for isomer production and from a change in dominant species of LCA producers.

4.8. Pollen data

The Yarkov-04 core was analyzed for pollen, spores, and non-pollen palynomorphs with a standard technology at the Institute of Archaeology and Ethnography SB RAS. The method of biomisation was used to quantify the dominant vegetation types, and a statistical reconstruction of annual precipitation was carried out; see Supplementary Data Text 1 for details.

Pollen zones.

The pollen data presented in the diagram (Fig. 9) covers the top 200 cm Layer 1; Layer 2 and the sub-basin loess-like sediments did not provide sufficient pollen grains per sample. The interval of reliable pollen data was divided into six pollen zones (PZ):

PZ I (200–190 cm, 3.6–2.9 ka BP). Scots pine and Siberian pine (*Pinus sylvestris* and *P. sibirica*) are dominant trees, spruce and fir (*Picea* and *Abies*) are subdominant in this zone; birch (*Betula* sect. *Albae*) is almost absent. Pollen of Amaranthaceae reaches 20 % and dominates in the group of herbs. Other herb taxa in the order of abundance are wormwood (*Artemisia*), grasses (Poaceae), sedges (Cyperaceae) and aster family (Asteroideae subfamily) plants. The distinctive feature of this zone is the stable presence of leadwort family pollen (Plumbaginaceae) at the level of 4 %.

PZ II (190–164 cm, 2.9–1.8 ka BP). Scots pine pollen dominates, up to 50 %, percentage of spruce and fir decreases, concentration of birch pollen becomes sizeable (1 %—3 %). Proportions of Amaranthaceae and Plumbaginaceae considerably decrease and those of wormwood, grasses and aquatic plants increase.

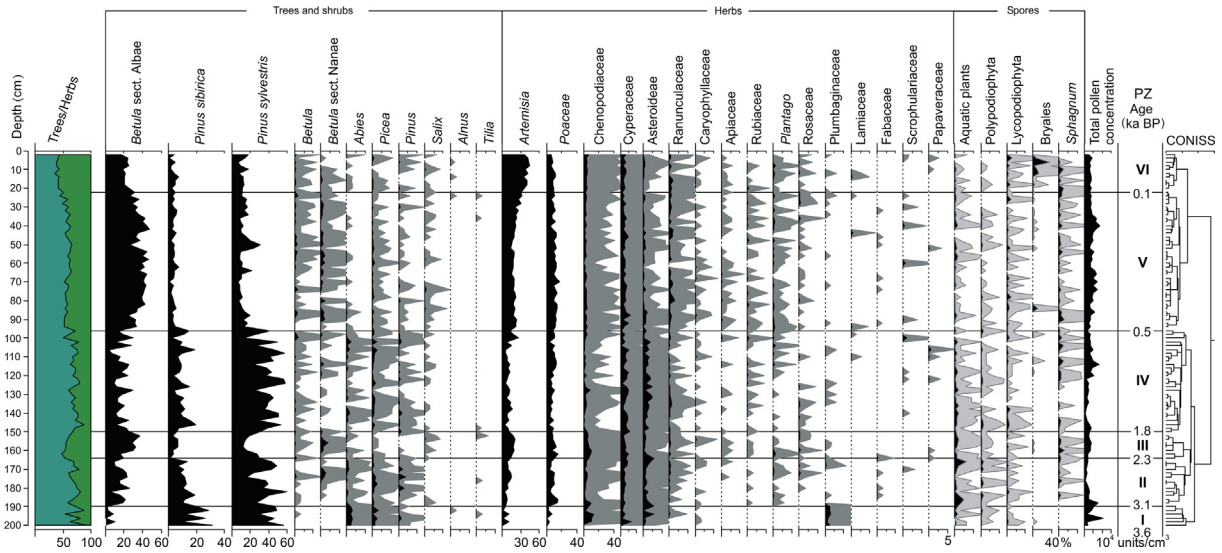

Fig. 9. Pollen diagram from Yarkov-04 core. Histograms filled by black color show pollen percentage. Histograms filled by grey color show the same percentage with exaggeration factor 5. PZ – pollen zones.

PZ III (164–150 cm, 1.8–1.4 ka BP). This zone shows increase of birch pollen up to 40 %; it becomes dominant and conifers proportionally decrease. Wormwood, grasses and chenopods increase and totally reach 50 %.

PZ IV (150–96 cm, 1.4–0.5 ka BP). Scots pine dominates again up to 60 % and proportion of Siberian pine is lesser than in PZ I. Herbs totally decrease to 30 %, while Asteroideae and sedges increase.

PZ V (96–22 cm, 0.5–0.1 ka BP). Birch dominates and proportion of pines decreases to 10 %—20 %. *Artemisia* rises to 20 % and grasses rise to 10 %; part of Amaranthaceae and Ranunculaceae pollen insignificantly increases and Asteroideae decreases.

PZ VI (22–0 cm, 0.1–0 ka BP). Proportion of trees and herbs changes and herbs become dominant, up to 60 %. Among them, wormwood reaches 50 %, Amaranthaceae increase and Asteroideae and Cyperaceae decrease.

Biome analysis.

Biomisation of the pollen data revealed three dominant biomes: taiga, cold deciduous forest, and steppe. The balance of taiga and steppe scores is indicative of the vegetation and climatic changes in the region of investigation (Fig. 10). Taiga dominated 3.6–1.9 ka BP (200–161 cm depth) and 1.6–1.0 ka BP (151–95 cm). Biomes of taiga and steppe were about equal 1.9–1.6 ka BP (161–151 cm) and 1.0–0.3 ka BP (95–28 cm). The apparent dominance of the steppe biome appears only since 0.3 ka BP to present.

Reconstruction of annual precipitation.

The highest values for PANN 464–440 mm/yr cover a period of 3.6–3.0 ka BP, 200–189 cm (Fig. 10). Precipitation gradually decreased 3.0–1.6 ka BP (189–151 cm) and then increased significantly. The relatively high PANN phase was between 1.6 and 1.0 ka BP (151–95 cm), after which the precipitation curve decreases. The curve has an average value of 380 mm/yr between 1.0 and 0.3 ka BP (95–28) cm; then the curve shows another decrease. Thus, the Yarkov data indicates humid conditions in the pollen zones PZ I, PZ II and PZ IV, mean PANN 427.5, 407.5 and 403.2 mm/yr, respectively, with maximum precipitation reaching 464.9 mm/yr in PZ I 3.6–3.0 ka BP. The driest conditions were in PZ III and PZ VI, 367 and 357.1 mm/yr, respectively.

4.9. Diatom data

The Yarkov-04 core was analyzed for diatoms with a standard technology at the Volga Region Federal University, Kazan, Russia. The diatom assemblages have been defined in terms of habitat and tolerance to water salinity, pH, temperature and rheophily of the species and their geographical distribution. See Supplementary Data Text 1 for details.

The diatom distribution in the lake basin sediments, examined in 35 samples from 2 to 243 cm in the core, showed two distinct parts delimited between samples with a depth of 140 and 150 cm: the upper part with diatoms and lower part without them (*Campylodiscus clypeus* was found in small amount in two samples at depth 222 and 210 cm). This means that diatoms inhabited the lake mainly in the stage represented by Sublayer 1a. There are also intervals without diatoms: samples at depth of 20 and 6 cm.

The diatom complex includes 27 species and varieties, 12 of them live in the Chany lake system now, see Supplementary Data Table S3. The diversity of diatoms is not high: the number of taxa in the samples ranges from one to eleven. The abundance of diatoms is generally very low; their appearance varies from 0.5 to 270.5 frustules per slide. These parameters are similar to the modern characteristics of Lake Chany, which diatom flora includes 24 species, and the total abundance of phytoplankton is negatively correlated with the water salinity (Kirillov et al., 2015). The complex consists mostly of cosmopolitan diatoms, 66.7 % of the total number of species. By habitat, it includes 59 % of benthic species. Most species of the complex are indifferent to temperature, rheophily, and salinity. In relation to pH, 51.9 % are alkaliphilic (Supplementary Data Table S4).

The diatom diagram (Fig. 11) infers two diatom zones (DZ):

DZ I (140–20 cm, 1.1–0.1 ka BP). The zone includes 22 species. The benthic boreal salinity and pH-indifferent *Campylodiscus hibernicus* is dominant and benthic mesohalobic *Campylodiscus clypeus* and planktonic halophylic *Campylodiscus echeneis* are subdominant.

DZ II (20–0 cm, 0.1–0 ka BP). Among the 16 species found in this zone, the benthic mesohalobic *Campylodiscus clypeus* is dominant and the planktonic-benthic salinity-indifferent *Aulacoseira granulata* is subdominant.

Reconstruction of the lake depth and salinity.

In DZ I, the major part of Sub-layer 1a, the diatom complex reflects a shallow-water basin with lower mineralization than now. The monodominance of *Campylodiscus hibernicus* in the intervals 122–112 and 78 cm suggests increases in water level and desalinization at 1.0–0.8 and near 0.4 ka BP, respectively. In DZ II, the upper 20 cm part of Sub-layer 1a, the diatom complex

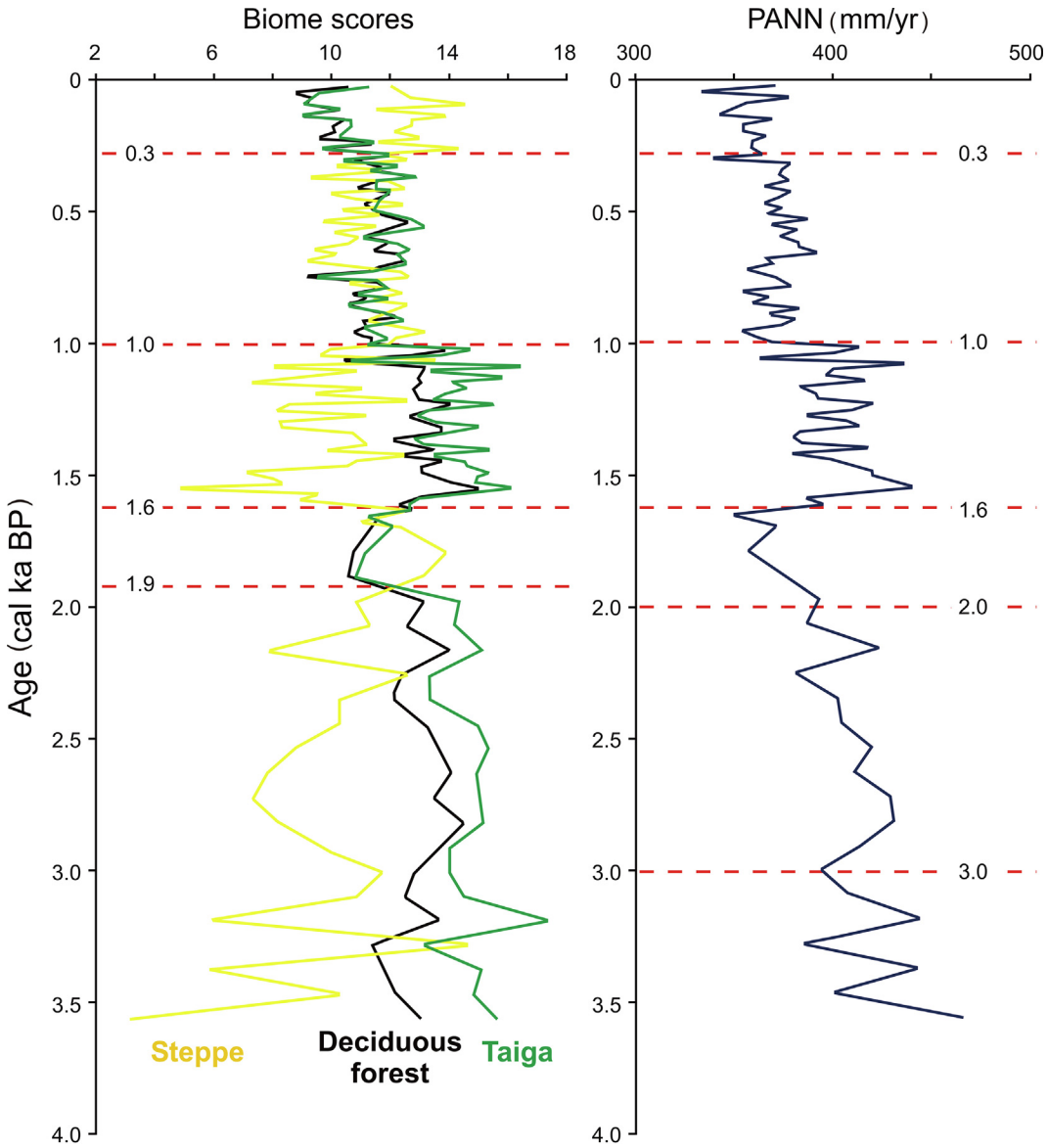

Fig. 10. Biome scores and PANN revealed from Yarkov-04 pollen data.

indicates larger than in the previous zone number of halophilic and mesohalobic planktonic and plankton-benthic species, which suggests a deeper and more saline lake.

4.10. Chironomid data

Treatment of the Yarkov-04 sediment samples for chironomid analysis and identification of the fossils followed standard techniques. Statistical interpretation was used to reconstruct the water depth and average July air temperature. See Supplementary Data Text 1 for details.

Chironomid zones.

Remains of chironomid larvae were found in 17 samples in the 0–200 cm interval of the core (Layer 1). Sediments below 200 cm did not contain chironomid remains. The fossils belong to 26 taxa from 21 genera and 4 subfamilies (Supplementary Data Table S5). *Chironomus plumosus*-type and *Cladotanytarsus mancus*-type were the most abundant taxa in the studied core, reaching maximum abundance of 60 % and 58.9 %, respectively. *Microchironomus* (max 25.5 %), and *Procladius* (max 27.6 %) also had high abundances throughout the core. *Cladotanytarsus mancus*-type is usually encountered in the littoral of warm and productive lakes and can tolerate acidic conditions. *Chironomus plumosus*-type, *Microchironomus* and *Procladius* usually occur in profundal of mesotrophic to eutrophic waters. However, *Chironomus plumosus*-type and *Procladius* are known for their tolerance to a broad spectrum of ecological conditions, including periods of anoxia, low pH. Some species from the *Chironomus plumosus*-type group tolerate high level of salinity (Stief et al., 2005; Golovatuyk et al., 2020, 2022). Both taxa can often be found in conditions unfavourable for other chironomid species and *Chironomus* species are often early colonizer of new environments or waters after significant ecological change (Brooks et al., 2007 and references therein). High representation of *Chironomus plumosus*-type throughout the core indicates possible permanent presence of anoxic or low-oxygen zones in the lake profundal and eutrophic state of the lake.

Sample scores of the first PCA axis showed that the chironomid assemblages of the upper (above 110 cm) and lower (below 110 cm) parts of the core differ markedly. Therefore the chironomid record was divided into two chironomid assemblage zones (CZ) (Fig. 12).

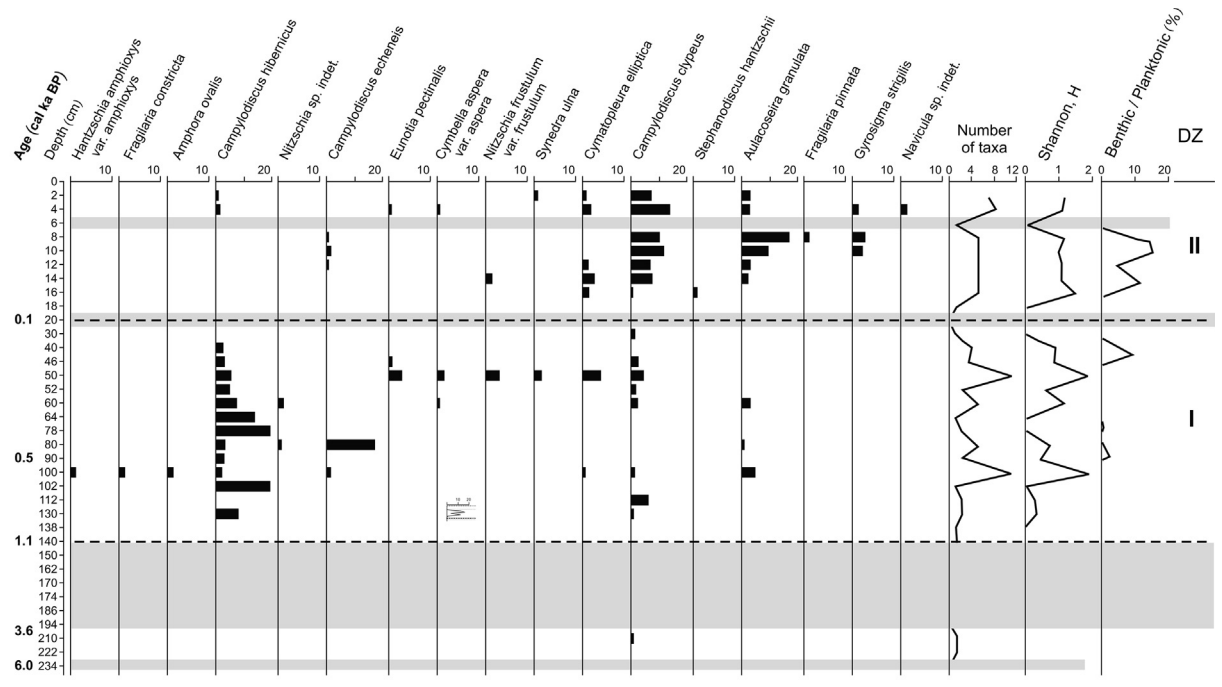

Fig. 11. Relative abundance (%) of diatom species, number of diatom species per sample, Shannon diversity index (H) and ratio of benthic to planktonic diatom species in Yarkov-04 core. Grey bars indicate intervals without diatoms; DZ - diatom zones.

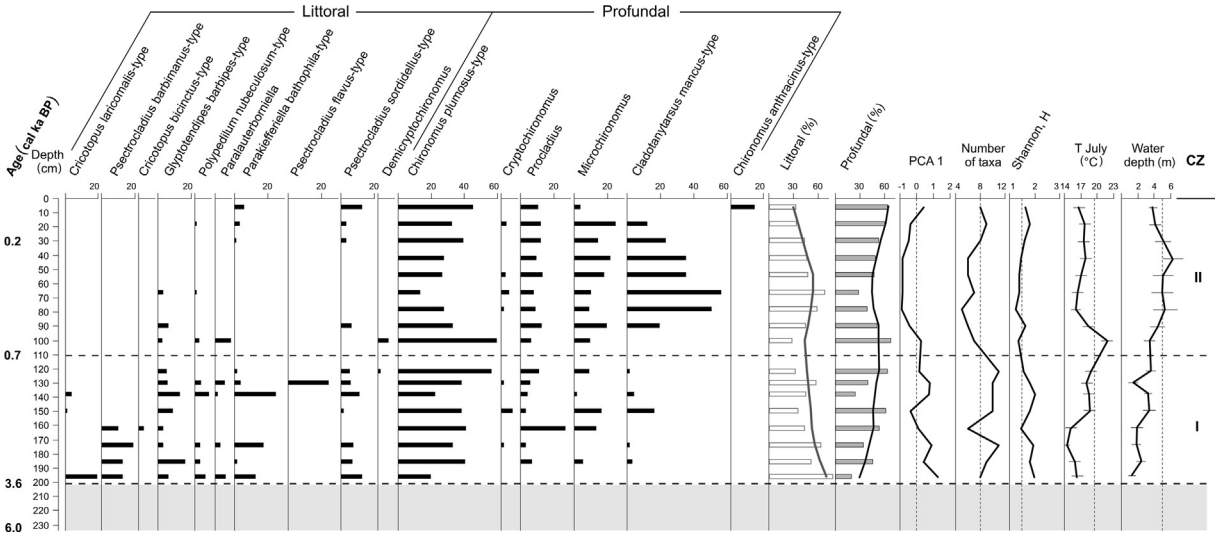

Fig. 12. Relative proportions of the most abundant chironomid taxa and profundal and littoral taxa (%), PCA axes 1 scores, number of taxa per sample, and Shannon diversity index (H) of chironomid communities, chironomid-inferred mean July air temperature (T July,℃) and water depth (WD, m) in Yarkov-04 core. Grey vertical dashed lines at the reconstructed T July and WD represent modern mean July air T (℃) and current water depth in the Yarkov sub-basin of Lake Chany. Grey horizontal lines at the reconstructed T July and WD represent estimated errors of prediction. Gray bar indicates an interval without chironomids; CZ - chironomid zones.

CZ I (200–110 cm, 3.6–0.7 ka BP). This zone shows high taxonomic richness, diversity and abundance of littoral chironomid taxa; on average 56.5 % are those that prefer shallow water conditions. A major part of the chironomid assemblages are taxa that currently live in temperate to warm conditions in the macrophyte-rich littoral zone of eutrophic lakes. The dominant *Chironomus plumosus*-type is tolerant to anoxia and low pH; some other *Chironomus* species are tolerant to salinity. *Glyptipendipes barbipes*-type, a submerged vegetation miner, is found in all samples with up to 17 % abundance. Several *Cricotopus* taxa and *Paralauterborniella* are related to vegetation (Brooks et al., 2007). Presence of three *Psectrocladius* taxa (*P. sordidellus*-type, *P. flavus*-type, *P. barbimanus*-type) at different levels of the zone is indicative of low pH in the lake littorals. The acidic conditions in the lake may be caused by paludification of the shore zone and decomposition of macrophytes and submerged vegetation at low lake level (Nazarova et al., 2017).

CZ II (110–0 cm, 0.7–0 ka BP). This zone shows a lower taxonomic richness of chironomid assemblages with an average of 6.5 taxa per sample. The taxonomic richness of profundal taxa

remains the same as in CZ I, but the richness of the littoral fauna declines from an average of 7.5 taxa per sample in CZ I to 4 taxa per sample in CZ II. The littoral *Cladotanytarsus mancus*-type, which is tolerant to acidic and brackish-water conditions (Epler, 2001; Brooks et al., 2007), reaches a maximum in the middle of CZ II (66 cm) and decreases towards the top of the zone. At the top of the zone (above 30 cm; after *ca* 0.17 ka BP), the abundances of the typical for eutrophic lakes *Parakiefferiella bathophila*-type and acidophilic *Psectrocladius sordidellus*-type, as well as the taxonomic richness of littoral fauna, is increasing.

The abundance of the dominant profundal *Chironomus plumosus*-type decreases in the middle part of the zone with a minimum at a depth of 66 cm (ca 370 ka BP). The *Procladius* shows slight variation throughout the zone and another dominant profundal taxon *Microchironomus* increases at the top of the zone with a maximum 25 % at, at a depth of 18 cm (ca 1.0 ka BP). The *Chironomus anthracinus*-type, found at abundance of 15 % at the sample from a depth of 6 cm (ca. 0.3 ka BP) has lower temperature optima than *C. plumosus*-type and may indicate some cooling.

Reconstruction of water depths.

In CZ I, the reconstructed water depth changed from 1.2 m at the bottom to 3.5 m at the top of the zone (2 m median depth is lower than now). A short-term decline of the level to 1.3 m of water depth is reconstructed for the 130 cm deep level of the core, ca. 1.2 ka BP, along with an increase in the representativeness and taxonomic diversity of the littoral taxa. In CZ II, the water depth reaches the modern depth of 5 m between 0.4 and 0.5 ka BP (78 and 90 cm) and remains stable up to ca. 0.17 ka BP with a short-term deepening to 6.4 m at ca. 0.24 ka BP. After 0.17 ka BP, the lake slightly shallowed to a depth of ca. 3.8 m at 0.03 ka BP (ca. 1920 CE).

Reconstruction of air temperatures.

In CZ I, the reconstructed TJuly varies between 14.0 and 15.7 ℃ till 2.2 ka BP (162 cm) and then rises to ca. 18 ℃ in the upper part of CZ I (1.8–0.7 ka BP) with a short-term 1 ℃ decline at 1.2 ka BP (130 cm). In CZ II, the reconstructed T_{July} ranges between 16 and 17.2 ℃; it was the highest at ca. 0.56 ka BP (100 cm) and lowered between 0.5 and 0.03 ka BP.

5. Discussion

5.1. Origin of the Yarkov sub-basin sediments from their environmental characteristics

Here we correlate the environmental events recorded in the Yarkov sub-basin identified by the proxy indicators; Fig. 13 integrates the data plotted against the timescale. The events found from certain proxies reflect the evolution of different components of the environment, and their changes do not necessarily coincide in time. Additionally, the proxies were derived from three different cores, correlated mainly by stratigraphy. In these circumstances, the correlation of the units in Fig. 13 looks quite good; only rock magnetic data show discrepancies, which may be a specific feature of magnetic signals or low accuracy of the correlation between the reference Yarkov-02 core and the Yarkov-03 core used for the magnetic study. The visual description of the sediments and their overall composition define two large layers with two sub-layers in each. Sub-layers 1b and 2a represent the sandy interval. The presence of sand suggests that sand is easily transported into the basin, thus excluding deep-water conditions for the interval. Overall, the boundary between Layers 1 and 2 dated at 3.6 ka BP is easily traced in the proxies. The deeper lake is reconstructed for the upper part of the sediments since ca. 1.5 ka BP. The lacustrine conditions are obvious for the 3.6–0 ka BP interval, i.e., Layer 1. The origin of the entire Layer 2 is unclear and poorly proven, as discussed below.

5.1.1. Pre-lake interval

Seventy-four centimetres of blackish silts of Layer 2 accumulated during 5.5 ka with sedimentation rate and sediment input 0.013 cm/yr, and 0.024 $g/cm^{2}*yr^{-1}$, respectively, which is very low compared to the values of Layer 1 (Table 3); however, there are other lakes that we have examined in southern Western Siberia, such as Itkul and Ebeity (Fig. 1B) Supplementary Data Table S6, which showed similar low sedimentation rates for definitely lake facies (Supplementary Data Table S6). Our sedimentological proxies do not clearly indicate origin of Layer 2 of the Yarkov. Other proxies mostly argue against a lacustrine origin rather than supporting it. There is an absence of chironomids and diatoms that require open water; only a small number of diatoms have been found in the upper part of Layer 2 (Fig. 13). However, diatoms are missing in the overlying Sub-layer 1b, representing the shallow-water lake. This detracts from the importance of diatoms as lacustrine indicators in the Chany basin. Additionally, Layer 2 showed a negligible amount of pollen (not enough for statistical interpretation), an unusual phenomenon, possibly related to poor conditions for pollen preservation. The lipid spectra of both *n*-alkanes and long-chain alkenones, despite their abundance, also give a vague interpretation of origin; *n*-alkanes suggest terrestrial lower plants and bacteria as their sources. The rock magnetic parameters showed the maximum concentration the of pedogenic (PD) component and the absence of the detrital and extra-cellular (D-EX) component; these are very close to the Holocene automorphic and semi-hydromorphic soils of the Barabinsk forest-steppe region (Matasova et al, 2016). The concentration and composition of authigenic Ca-minerals testify a low-salinity sedimentation environment with low-grade precipitation of low-Mg calcite from medium-carbonate and moderately saline water. Both C and O carbonate isotopes indicate mainly a meteoric source of the water. As a result, a huge lake is unlikely for the 20x20 km wide Yarkov sub-basin in the period of 9.1–3.6 ka BP. These data infer a "swampy" or muddy landscape changeable in space and in time (seasonally), which water supply was mainly atmospheric precipitation. Such a water-meadow landscape (*zaymishche* in Russian) is widespread in central Baraba and especially around Lake Chany. A distinctive feature is the abundance of perennial reed grasses *Phragmites*, but this is not confirmed for our reconstructed Yarkov sub-basin Layer 2 environment. On the other hand, the pedogenic process inferred from the rock magnetic data is not obvious from the sedimentological description.

5.1.2. Lake interval

The upper 200 cm thick Layer 1 clearly indicates a lacustrine environment since 3.6 ka BP (Fig. 13). It includes shallower-water Sub-layer 1b and deeper-water Sub-layer 1a with much higher sedimentation rates and sediment inputs for the latter (Table 3). The sediment input was 3 and 7 times higher, respectively, than in the pre-lake Layer 2. The values are high and extremely high for the shallower and deeper-water facies, respectively; this differentiates Yarkov from other West-Siberian lakes we have surveyed (Supplementary Data Table S6). From the sedimentological data, the shallower-water facies is sandy and rich in ostracod shells; the transition to the deeper-water facies took place 1.5 ka BP. Generally, the sediment composition shows a gradual increase of the proportion of authigenic and organic components in the lacustrine part (Fig. 3).

The distribution of Ca-minerals across the core infers a geochemically matured lake above the boundary of 3.6 ka BP, with variable Ca-mineral composition and gradual increase in water mineralization, which seems normal for endorheic Lake Chany. The C and O stable-isotope values are high for the lacustrine stage and clearly indicate periods of shallower and deeper lake conditions. The rock magnetic data suggest a changeable environment

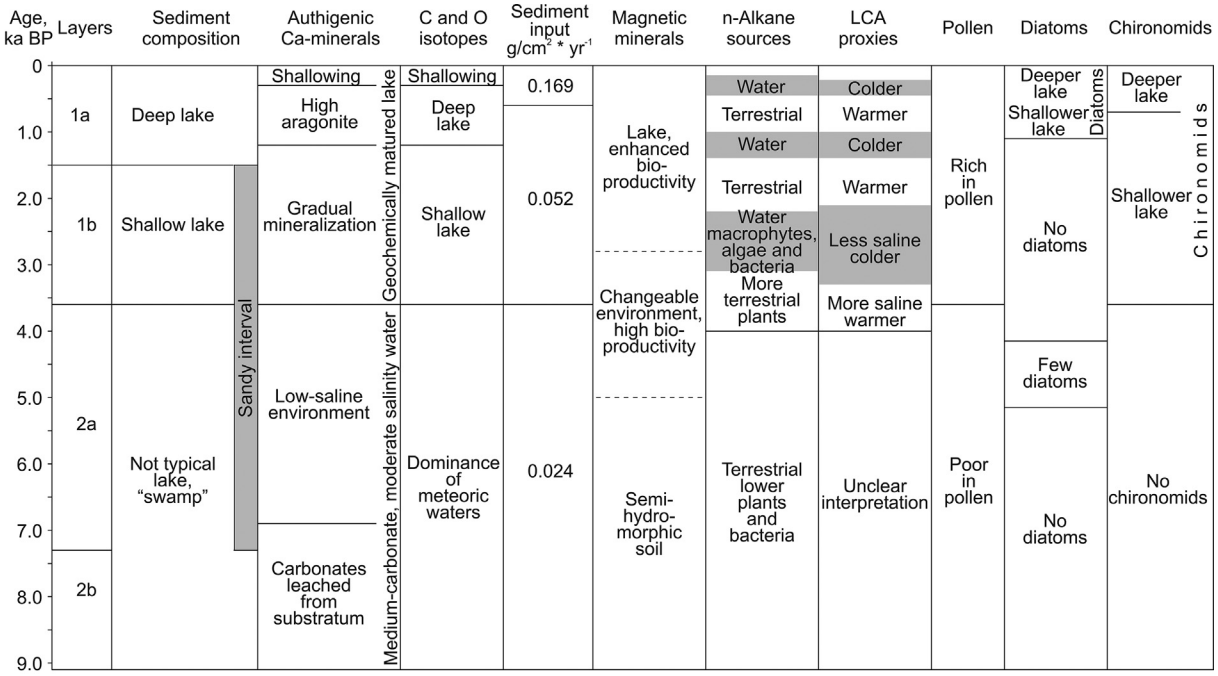

Fig. 13. Correlation of environmental changes recorded in the Yarkov sub-basin.

and high bioproductivity in a long transition zone between Layers 2 and 1 (validity of the boundaries is discussed in Section 5.1) leading to the establishment of a permanent lake. The lipid biomarker data confirm the lake's state after ca. 4 ka BP, and show several fluctuations in the lipid sources: the prevalence of water macrophytes, algae and bacteria, or, in addition to the above, a higher proportion of terrestrial plants. These differences are interpreted as less saline (colder and wetter), and more saline (warmer and drier) conditions, respectively, without reference to water depth.

The lacustrine part is rich in pollen, including aquatic plants. The proportion of aquatic plants is higher in the shallower-water facies and lower in the deeper ones. Diatoms are absent in the shallower-water facies and present in the deeper lake interval since 1.1 ka BP. In the latter, diatoms indicate shallower and deeper lake facies; the deeper part spans only the last 0.1 ka. Chironomids are present throughout the whole lake sediments and identify shallower and deeper parts with the boundary at 0.7 ka BP.

In summary, the whole dataset supports the general trend of the lake development towards deepening and salinization. A transition from a shallower to a deeper lake started no earlier than 1.5 ka BP. Salinity generally increased, despite the increase in water volume.

5.2. Refining the details of the lake stages

The proxy data (Fig. 14) provide further insight into the development of the Yarkov sub-basin and the whole of Lake Chany during the last 3.6 thousand years. Against a backdrop of fairly harmonic general trends, some proxies show variations in depth and salinity. The depth-change model based on the chironomid data shows a gradual increase in water depth with a short-term drop at about 1.2 ka BP. The rise in lake level was small from 1.2 to 3.5 m until 0.7 ka BP and then increased dramatically to ca. 6 m, which coincides with the depth of the Yarkov sub-basin today. The maximum depth of 6.4 m is recorded at 0.24 ka BP with a subsequent shallowing trend.

The biomarker data show that two types of lake conditions alternate in terms of salinity of water (LCA) and proportion of lipids of terrestrial plants versus water macrophytes, algae and bacteria (*n*-alkanes) (Fig. 14). The data indicate a concomitant increase in the water salinity and in the proportion of terrestrial plants, or, more precisely, a decrease in the aquatic plants, presumably as a result of adverse salinization. The data indicate four salinization events and three less saline events during the last 3.6 ka; these can be interpreted as the lake water level decreasing and increasing, respectively. The record is quite detailed compared to other discussed proxies but is not well matched by trends in the other proxies. We suggest that it correlates better with paleoclimatic proxies than with those recording lake ecology.

The recent shallowing of the lake is supported by the mineralogical, isotope and chironomid data. The Ca-minerals and isotopes show shallowing since about 0.3 ka BP, and chironomids since 0.24 ka BP. The shallowing is also recorded in the lipid biomarkers as warmer, drier and more saline episode with higher input of terrestrial plant matter. However, the decrease in the authigenic component of the sediments since 0.1 ka BP (Fig. 3) indicates desalinization instead. Notably, the diatoms, which suggest a deeper and more saline lake in recent times, do not contradict other proxies: at this point, the lake is enough deep for diatoms. Diatoms appeared about 1.1 ka BP, when the lake began to rise. The absence of diatoms at depths of 20 and 6 cm we explain by post-sedimentational dissolution of biogenic silica in the Ca-rich geochemical environment of the lake (Flower, 1993).

5.3. Paleohydrological explanation for delay in Lake Chany rise

A previous study showed the specific role of the Chany basin catchment topography in the lake's water supply (Krivonogov et al., 2018). Water flowing into Lake Chany via the Chulym and Kargat rivers (Fig. 1B) accounts for 45 % of the total water budget of the lake (Savkin et al., 2006). Therefore, any change in river input could influence lake level. Today, the rivers flow through chains of saucer-shaped basins, which are swampy meadows and two of them, the closest to the Chany, are drainage lakes (i.e., lakes drained by an outlet stream). Previously, between 6.3 and 2.0 ka BP, all these basins collected water of the Kargat and Chulym rivers

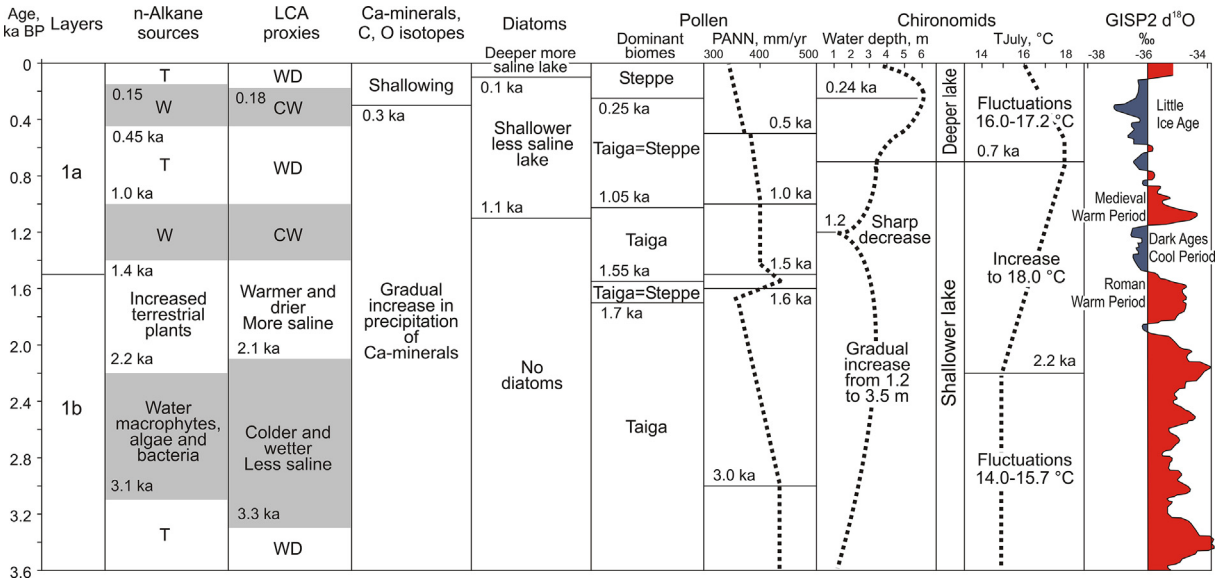

Fig. 14. Finer correlation of lacustrine and climatic events. Abbreviations for *n*-alkane sources: T – increased terrestrial plants; W – water macrophytes, algae and bacteria. Abbreviations for LCA proxies: WD – warmer and drier; CW – colder and wetter. Dominant biomes: Taiga = Steppe – two dominant biomes in equal proportion. GISP2 d^{18}O graph is modified from Easterbrook (2016).

and served as intermediate lakes, which reduced or even blocked the runoff to the Chany.

GIS calculated total water capacity of these basins is equal to 7.5–4.5 times the modern annual runoff of the Chulym and Kargat rivers. Additionally, the estimated annual evaporation from the surface of these lakes could exceed modern annual runoff of the rivers.

The lakes sequentially disappeared because of erosional lowering of their drainage thresholds and their filling by sediments, which, together with decrease in their surficial evaporation, should steadily increase the runoff. Thus, we assumed that there could be no river inflow into Chany Lake in the early stages of its development, and, when it appeared, it was reduced until 2 ka BP.

5.4. Paleoclimatic interpretation

Paleoclimatic information is derived from the pollen, chironomid and biomarker data (Fig. 14). The pollen-based biome scores from the Yarkov core show distinct fluctuations probably reflecting climatically-driven shifts in the vegetation boundaries: taiga/forest-steppe in the north and steppe/forest-steppe in the south. The taiga scores are higher in wetter periods, and steppe scores in the drier, according to the PANN proxy. The chironomid-based T_{July} reconstruction yielded slightly lower values, as the current mean July temperature in the region is +19 ℃. It shows relatively low temperatures between 3.6 and 2.2 ka BP followed by a gradual increase with a maximum value ca. 0.7–0.4 ka BP, and a subsequent decrease. The LCA biomarker proxies revealed three colder and wetter episodes at 3.3–2.1, 1.4–1.0, and 0.45–0.15 ka BP.

A comparison of the LCA, PANN, and T_{July} curves from the Yarkov shows the correspondence of warmer periods to drier ones, and vice versa colder to wetter. This is consistent with data from the adjacent regions of arid Central Asia, north of the Tibet Plateau (e.g. He et al., 2013), i.e., it aligns with a widespread intracontinental pattern.

In comparison with the overall climate change in northern hemisphere as represented by the Greenland (GISP2) oxygen isotope curve (see Fig. 14), summer sea-surface temperatures near Iceland, and a temperature reconstruction from tree rings in China (overviewed in Easterbrook, 2016) our data does not show strict correlation of warmer and colder events. First of all, the paleoclimatic proxies of Yarkov undoubtedly indicate colder conditions in the region prior to 2.0 ka BP which disagrees with the GISP2 data evidencing warming. The later hemispheric short-term warming and cooling events are well recognizable in the biomarker proxies of Yarkov. Its pollen-based proxy yielded less matching result, and the chironomid-based data completely contradicts GISP2. Therefore, the applicability of the Yarkov paleoclimatic data requires further argumentation.

5.5. Regional review of lake histories of south-western Siberia

Several comprehensive studies of the region's lakes over the past two decades have enabled us to compare their main characteristics, such as sedimentation patterns, level changes, and related climate changes, in order to highlight the consistency and inconsistency of their development. We describe the lakes in north–south order, which shows their geographic differences. This review is useful for a better understanding of the features of Lake Chany, located in the middle of the region, and improves the regional perspective on environmental change.

5.5.1. Sedimentation and level changes

The lakes of the forest-steppe and steppe zones of the region (Fig. 1B) have different types of sedimentation: organic and organic-mineral in the north, and mineral and mineral-authigenic in the south (e.g. Maltsev et al., 2019). The more northerly lakes accumulate organic-rich sapropelic sediments rapidly. Lakes in relatively shallow depressions are not deep and almost filled (compensated) by sediments (e.g. Beloye and Bolshie Toroki, Supplementary Data Table S5). Those with deeper depressions are not fully compensated and are relatively deep in their central parts (e.g. Kirek and Minzelinskoye). We suggest that, in general, all these lakes should raise their level through sedimentation. However, as some of the investigated lakes are exorheic (Beloye, Kirek, and Minzelinskoye) they lose excess water via outlet streams and their levels are fairly stable. Sediments indicate that the northern sapropelic lakes were shallower at an early stage of development, when peaty sapropel formed, and deeper later, when water-macrophytic sapropel formed. This change is not

synchronous and occurred in different lakes between 6 and 3.4 ka BP. This suggests that changes in sedimentation in these lakes more reflect site specific processes (e.g. vegetation successions) and less climate change.

Lake Itkul (Fig. 1B) represents sedimentation environment in the middle region, and is similar to the Yarkov sub-basin of Lake Chany. In contrast to the latter, Itkul is almost a freshwater lake and has an outlet to the Chulym River that is active during the highest stands; these are marked by a wave-cut cliff 2 m above the modern level (Maltsev et al., 2020). The lake has organic-mineral sedimentation that has not changed during the 8.2 ka of its history. However, the western almost separate bay of the lake has biogenic sedimentation. The bay was wetland and swamp 8.5–5.8 ka BP. This means that the bay and the main part of Itkul have long developed as separate water bodies. They became one lake at 3.8 ka BP, which reached its highest level at about 3 ka BP.

Lake Sargul (Fig. 1B) belongs to a system of intermediate basins in the Lake Chany catchment. Water of the Chulym River transits the lake, which serves as one of several river-water collectors on the way to Lake Chany (Krivonogov et al., 2018). The lake was formed 8.7 ka BP and for a long time was large enough to form an extensive sandy terrace dated at ca. 3.5 ka BP near its surface. The sediments of the sand terrace are rich in fossils: mollusc shells and ostracods, and, curiously, foraminifers that share identity with those of the Aral Sea (Gusskov and Yadrenkin, 2000); this remains an unsolved paleogeographic problem (Krivonogov et al., 2008; Gus'kov et al., 2011; Riedel et al., 2011). Later, the lake shallowed and deposited sapropelic mineral-organic and organic-mineral sediments.

Low saline Lake Malye Chany (Fig. 1B) is a part of the Chany lake system. It takes the waters of the Chulym and Kargat rivers and transmits them further to the main Lake Chany via a channel. The lake sediments consist of two parts: sandy deposits representing an underwater delta of the Chulym River that was active ca. 6.7–4.0 ka BP, and sapropels, which are clearly lacustrine (Khazin et al., 2016). The lake became a peat bog for a short period about 3.1 ka BP, and the deeper-water environment was established only 1.9 ka BP.

Endorheic Lake Maloye Yarovoye is located south of the Chany in the plains of the Steppe Altai Territory (Fig. 1B). It has a rather small catchment and a salinity of 180–280 g/L. However, the lake is quite deep, up to 5 m, and its current level is close to maximum. The 4.5 m thick lake sediments formed from 12.9 ka BP onward, and reflect variations in the lake water level and salinity (Rudaya et al., 2020). The lake was shallower before and deeper after 6.6 ka BP. Significant drying recorded in a salt layer occurred ca. 10.2–10.0 ka BP; other larger decreases occurred at about 5.7 and 3.5 ka BP, and smaller decreases at about 2.5 ka BP and at present.

Endorheic Lake Kuchuk, in the Steppe Altai, is terminal for the system of the Kulunda River, which transits via a large brackish-water Lake Kulundinskoye (Fig. 1B). The Kuchuk has a salinity of up to 320 g/L and a thick (up to 3 m) mirabilite layer in the bottom. The lake developed 13.7 ka BP and was deep enough to erode its shores and accumulate sandy-loam layers during most of the Holocene (Rudaya et al., 2020). Gradual salinization and parallel shallowing of the lake caused the mirabilite accumulation since ca. 5.5 ka BP, and the main salt layer formed between 4.3 and 1.6 ka BP. The surface organic-rich sediment reflects a recently increased planktonic production.

In summary, those lakes of the West-Siberian south that are so far studied demonstrate a variety of sedimentary environments, from predominantly biogenic to mostly authigenic, reflecting their climatic-geographical position. Their own histories, which differ from one lake to another, depend to a large extent on the local water supply and how they are filled with sediments. The sapropelic lakes in the northern part of the forest-steppe zone usually started as wetlands or peatlands. Their peaty and macrophytic sapropel stages mark an increase in the amount of water with time; however, the main facial changes were not synchronous from place to place. Overall increases of lake level may also result from the filling of the lake basins with sediments. The organic-mineral lakes of the southern forest-steppe, that is, the Lake Chany zone, are still poorly investigated; the known histories of Lake Itkul and Lake Malye Chany indicate a considerable increase in their levels in the late Holocene which resembles the history of Lake Chany (Section 5.1). The lakes of the steppe zone show variability in lake level throughout their history, but they have been generally relatively high in recent times.

5.5.2. Climate changes

Reconstructions based on LPAZ

The reconstructions illustrate differences in afforestation and steppification of the region (Supplementary Data, Fig. S1). The northernmost Lake Kirek, south of the southern taiga, yielded a record since approximately 8.3 ka BP, and showed an increase in conifers and waterlogging in the interfluve territory (Blyakharchuk, 2003). Unlike the taiga, where conifers are typical components, their increase in forest-steppe LPAZ indicates trends towards cooling and wetting, which contrasts with increase in steppe elements indicative of warming and drying.

In the northern forest-steppe, Lake Bolshiye Toroki shows expansion of conifers from 8 to 6.7 ka BP, and steppification 6.7–4.5 ka BP followed by afforestation; the modern birch dominated assemblages formed 1.8 ka BP (Zhilich et al., 2017). Closer to the modern southern taiga, Lake Beloye appeared about 6 ka BP records a high proportion of pine, which probably reflects features of local vegetation (Krivonogov et al., 2012a,b). A significant shift to cooling is indicated by the appearance of dwarf birch 3.4–2.3 ka BP and the probable paludification of the lake basin.

In the middle-to-southern forest-steppe zone, to which the Chany Basin belongs, we see local differences in afforestation and steppification. More northerly Yarkov sub-basin (this paper) showed a significant afforestation 3.6–0.9 ka BP and subsequent steppification. Both Yarkov and Lake Malye Chany (Zhilich et al., 2016) sites indicate the emergence of pine forests 3.6–3.3 ka BP. Yarkov records dominance of pine 2.2–0.9 ka, and Malye Chany afforestation 2.1–1.8 ka BP; these events appear broadly correlative. Lake Ebeity, further west and south, also showed afforestation 2.8–0.9 ka BP correlative with that of the Chany Basin (Zhilich et al., 2015); however, the Ebeity region experienced recent afforestation, unlike the Chany basin.

In the eastern part of the steppe zone, lakes Maloye Yarovoye and Kuchuk consistently show that pine forests were and remain components of the steppe landscapes of the region (Rudaya et al., 2020); these are ribbon-like pine forests that occupy river valleys in the eastern part of the Steppe Altai region (Fig. 1B). The maximum cover of wooded vegetation occurred 7.3–2.7 and 7.1–1.2 ka BP, respectively. Westward, Lake Bolshoye Yarovoye, located close to the dry steppes of Kazakhstan, paradoxically shows a gradual increase in tree pollen, with a maximum at 2.5–0.2 ka BP, while steppe is the modern LPAZ (Rudaya et al., 2012; Kosareva et al., 2022).

Biome-based reconstructions

The biome curves insight into the downcore pollen changes, as they relate to the relative dominance of vegetation formations, or biomes (Fig. 15). The dynamic between steppe and forest is challenging to interpret, and surface levels were used as a key for understanding these changes. Changes among biome scores are not absolute, but their variation indicates the relative degree of afforestation or deforestation in the region.

The record from Lake Bolshiye Toroki (Zhilich et al., 2017), in the northern forest-steppe, shows three dominating biomes: in

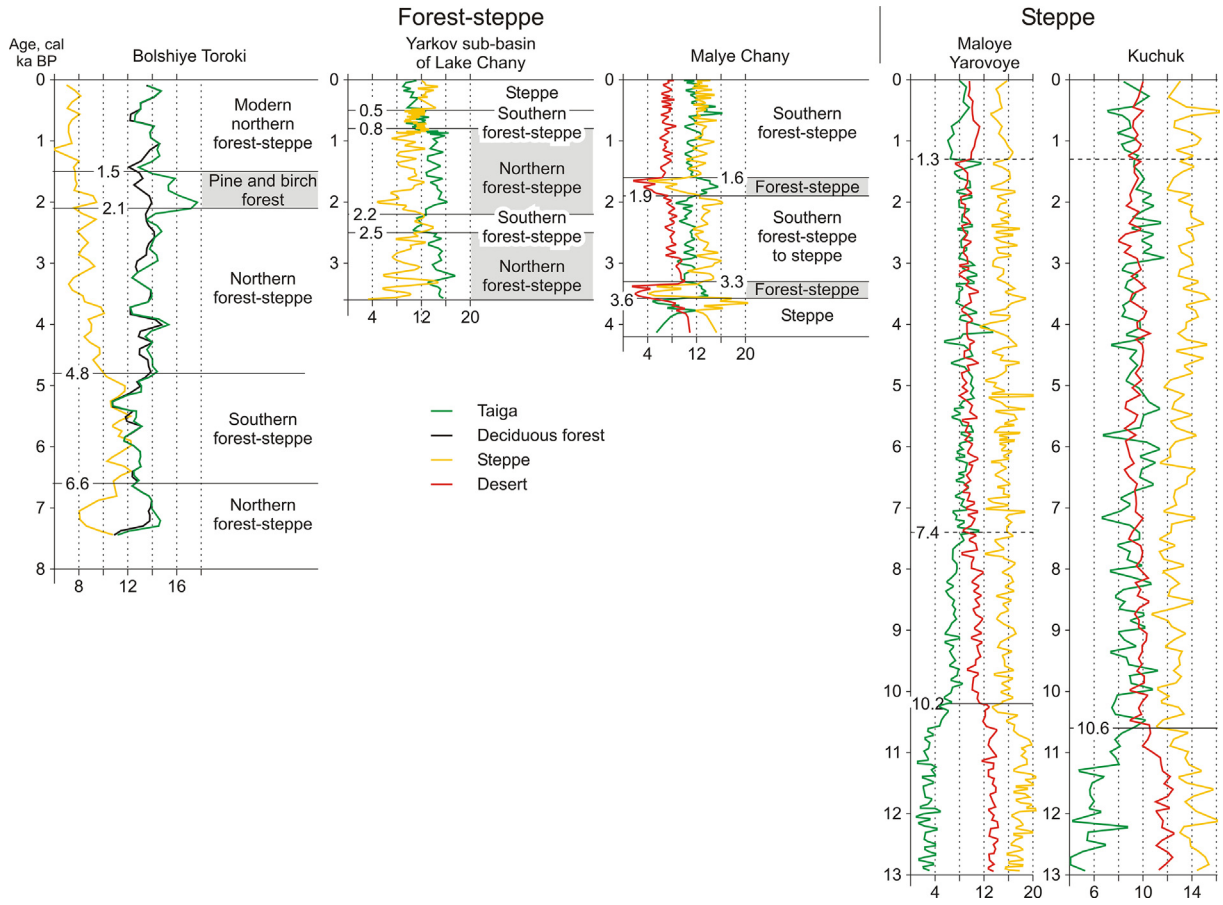

Fig. 15. Correlation of published vegetation change reconstructions for the region of investigation based on biome data. References are in the text.

order of significance, taiga, deciduous forest, and steppe. The first two vary in concert but show negative correlation with steppe. Here, the surficial level shows a considerable difference between the steppe scores and the two forest biomes interpreted to represent northern forest-steppe. This environment we see in the 1.5–0 ka BP and 4.8–2.1 ka BP intervals and prior to 6.6 ka BP. The taiga scores increased 2.1–1.5 ka BP, which suggests higher amounts of forest cover, whereas the higher steppe values and lower forest values 6.6–4.8 ka BP we interpret as southern forest-steppe.

Southward, in the Yarkov sub-basin of Lake Chany, in the middle forest-steppe, the dominant biomes represent fluctuations between taiga and steppe (Zhilich et al., 2016). Steppe predominated in the interval of 0.5–0 ka BP. This appears to be a mismatch with the modern vegetation around the sub-basin, which has quite high forest cover. Possibly, modern pollen spectra may have an increased steppe component that reflects vegetation of the saline landscapes surrounding the brackish-water Yarkov sub-basin and thus not reflect more regional patterns. Downcore, the biome characteristics are southern forest-steppe 0.8–0.5 and 2.5–2.2 ka BP, and northern forest-steppe 2.2–0.9 and ca. 3.6–2.5 ka BP.

Lake Malye Chany, located about 50 km further south, close to the southern forest-steppe, shows three dominant biomes: steppe, taiga, and desert (Zhilich et al., 2016). The biome scores identify the spread of southern forest-steppe landscapes 1.6–0 and 3.3–1.9 ka BP. More northern forest-steppe occupied the locality for short intervals of 1.9–1.6 and 3.6–3.3 ka BP and correlate with that of Yarkov. The lowermost part of the Malye Chany record indicates steppe and thus drier climate conditions.

Biome records from Maloye Yarovoye and Kuchuk lakes, in the steppe zone, show uniform changes of steppe, desert, and taiga biomes (Rudaya et al., 2020). The high steppe and desert scores and low taiga in the interval of 13–10.2 (10.6) ka BP most likely indicate the dry environment and periglacial steppe vegetation of the late glacial and their continuance in some form into the early Holocene. Subsequent Holocene vegetation was steppe. Lake Maloye Yarovoye indicates continuing low taiga values 10.2–7.4 ka BP. Both lakes showed decrease in taiga and increase in desert biomes 1.3–0 ka BP.

Paleoclimatic indices

The additional pollen-based paleoclimatic proxies are mean July air temperature (MTWA) for the Bolshiye Toroki Lake (Zhilich et al., 2017) and mean annual precipitation (PANN) for Yarkov (this study) and Maloye Yarovoye and Kuchuk lakes (Rudaya et al., 2020). The Bolshiye Toroki MTWA curve is mostly in the range of the local modern July temperatures with two intervals of higher-than-modern temperatures ca. 7.2–5.5 and 4.7–4.3 ka BP. Both peaks match the increase in steppe biome scores 7.3–4.5 ka BP.

The PANN data shows high precipitation 7.3–2.6 and near 1.3 ka BP at Maloye Yarovoye and 7.2–1.2 ka BP at Kuchuk. This matches slight increase of the taiga biome scores. The humid events of Yarkov (3.6–1.8 and 1.4–1.5 ka BP) match the humidity peaks described above.

6. Conclusions

The data from the Yarkov sub-basin of Chany Lake provide valuable information for better understanding the lake evolution and history of the whole Chany lake system. The sedimentological, mineralogical, rock magnetic, biomarker, and paleontological data are unequivocal evidence of the late (ca. 3.6 ka BP) appearance of

Chany Lake as a water body. Prior to this, the basin was a "swampy" landscape with very low sedimentation over ca. 5.5 ka: the pre-lake phase. During the lake phase, it was mostly shallower 3.6–1.5 ka BP; it became larger and deeper, similar to modern conditions, only in the last millennium. This is the "macro-evolution" of the lake. Observed seasonal, decadal and centennial climate-related fluctuations are somewhat unevenly represented in sediments and cannot yet be described, but they are potentially interesting and should be looked at further.

The history of Yarkov is similar that of Lake Malye Chany, which is a member of the Chany lake system as well. Malye Chany was not a typical lake prior to 3.6 ka BP; possibly the formation of the Chulym River sandy delta in the center of the lake and the later organic-rich sapropelic layer reflects a shallower lake until 2.5 ka BP and a deeper lake subsequently. Therefore, we observe common trends in the development of both lakes, and the timing differences may reflect the complexity of the development of the whole lake system.

We link this peculiar development of the Chany lake system with the specific topography of its catchment: the valleys of the inflowing rivers Chulym and Kargat include intermediate basins, which were transient lakes and for a long period captured most, if not all, river water (Krivonogov et al., 2018). This intensive blocking of the discharge to Lake Chany lasted ca. 8–2 ka BP. The data from Yarkov give more evidence for late release of catchment water into Lake Chany.

Climate probably also controls evolution of the Chany lake system. The pollen-derived paleoclimatic data for the region are useful for understanding environmental changes around Chany Lake during the 9 ka period of its development. All the data indicate predominance of forest-steppe landscapes with recurring trends toward northern and southern forest-steppe, or sometimes to steppe. The period of 9.1–3.6 ka BP, when the pre-lake part of the Yarkov sub-basin sediments formed, the environment can be inferred from the records of Lakes Bolshiye Toroki and Malye Chany. The evidence indicates that prior to 3.6 ka BP conditions were quite dry, and the subsequent increase in moisture was large and fast, which could have accelerated the filling of Chany Lake. Subsequent climatic events probably did not greatly influenced lake evolution, as the lake was shallow until 1 ka BP, and the subsequent abrupt rise of the water level is correlated with steppification events, not a moisture increase. This also implies a dominance of hydrological catchment factors in the evolution of Lake Chany over the climate.

Declaration of Competing Interest

The authors declare that they have no known competing financial interests or personal relationships that could have appeared to influence the work reported in this paper.

Acknowledgments

As the data presented in this paper have been collected and treated during more than 15 years, we acknowledge all funds and organizations supported the authors in this period. The paper is written within the State assignment of the Institute of geology and mineralogy SB RAS. The biomarker analysis and all organic matter related interpretations were made in favor of the joint Russia-China research project, RFBR no. 21-55-53037 and NSFC no. 42111530031. The lake level changes were investigated in favor of the RFBR project No. 19-29-05085. Numerical reconstruction of climate was made in the frame of ANSO Collaborative Research (ANSO-CR-PP-2021-02). The contribution by Natalia Rudaya matches interests of the RSF project no. 20-17-00110 and the Tomsk State University Development Program (Priority-2030). Xianyong Cao was financed by National Natural Science Foundation of China (grant no. 41988101) and the Sino-German Mobility Program (grant no. M-0359). Diatom and chironomid analyses were funded by the RSF project No. 20-17-00135. Databases developed with the support of the RSF No. 22-17-00185 and 22-17-00113 projects were used for quantitative environmental reconstructions (WD and T July) and supplementary statistical research. We acknowledge Dr. Kim Ju Yong, Korean Institute of Geosciences and Mineral Resources (KIGAM), for his kind help with radiocarbon dating. We are grateful to the reviewers Prof. Frank Riedel, Free University of Berlin, and Prof. Mary Edwards, University of Southampton, for their significant comments and improvements.

Appendix A. Supplementary data

Supplementary data to this article can be found online at https://doi.org/10.1016/j.gsf.2022.101518.

References

Blyakharchuk, T.A., 2003. Four new pollen sections tracing the Holocene vegetational development of the southern part of the West Siberian Lowland. The Holocene 13 (5), 715–731.

Brooks, S.J., Langdon, P.G., Heiri, O., 2007. Using and Identifying Chironomid Larvae in Palaeoecology. QRA Technical Guide No. 10. Quaternary Research Association, London.

Dunlop, D.J., 2002. Theory and application of the Day plot (Mrs / Ms versus Hcr / Hc) 2. Application to data for rocks, sediments, and soils. J. Geoph. Res. 107 (B3), 1–15.

Easterbrook, D.J., 2016. Using Patterns of Recurring Climate Cycles to Predict Future Climate Changes. In: Easterbrook, D.J., (Ed.), Evidence-Based Climate Science (Second Edition). Data Opposing CO_2 Emissions as the Primary Source of Global Warming, Chapter 21, Elsevier, pp. 395-411.

Egli, R., 2004. Characterization of Individual Rock Magnetic Components by Analysis of Remanence Curves, 1. Unmixing Natural Sediments. Studia Geophys. Geodaet. 48, 391–446.

Ermolaev, V.I., Vizer, L.S., 2010. Recent ecologic state of Lake Chany (West Siberia). Geogr. Nat. Res. 2, 40–46 (In Russian with English summary).

Ermolaev, V.I., 1998. Phytoplankton of large Chany-Baraba lakes in the south of Western Siberia, its species diversity and taxonomic structure. Siberian Ecolog. J. 5 (2), 137–145 (In Russian).

Flower, R.J., 1993. Diatom preservation: Experiments and observations on dissolution and breakage in modern and fossil material. Hydrobiologia 269 (270), 473–484.

Golovatuyk, L., Zinchenko, T.D., Nazarova, L.B., 2020. Macrozoobenthos community in saline Bolshaya Samoroda River (Volgograd region of Russian Federation): species composition, density, biomass and production. Aquat. Ecol. 54 (1), 57–74.

Golovatuyk, L.V., Zinchenko, T.D., Prokin, A.A., Nazarova, L.B., 2022. Biodiversity, distribution and production of macrozoobenthos communities in the saline Chernavka River (Lake Elton Basin, Russia). Limnology doi:10.1007/s10201-021-00692-w.

Grunert, J., Lehmkuhl, F., Walther, M., 2000. Paleoclimatic evolution of the Uvs Nuur basin and adjacent areas (Western Mongolia). Quat. Int. 65 (66), 171–192.

Gusskov, S.A., Yadrenkin, A.V., 2000. The first Holocene Foraminifera from the southern West Siberia. Novosti paleontologii I stratigrafii (Addenda to the Russian Geol. Geoph. 41) 2–3, 205–209.

Gus'kov, S A., Zhakov, E. Yu., Kuz'min, Ya.V., Krivonogov, S.K., Burr, G.S., Kanygin, A. V., 2011. New data on evolution of the Aral Sea and its relations with the West Siberian plain through the Holocene. Doklady Earth Sci. 437 (2), 460–463.

He, Y., Zhao, C., Wang, Z., Wang, H., Song, M., Liu, W., Liu, Z., 2013. Late Holocene coupled moisture and temperature changes on the northern Tibetan Plateau. Quat. Sci. Rev. 80, 47–57.

Ioganzen, B.G., Krivoschekov, G.M. (Eds.), 1986. Ecology of Lake Chany. Nauka, Novosibirsk (In Russian).

Kazantsev, V.A., Bulatov, V.I., Rotanova, I.N., Ustinov, M.T., Magaeva, L.A., Kurepina, N.Y., 2015. Chapter 2. Soil, Vegetation and Landscape. In: Vasiliev, O.F., Veen, J. (Eds.), 2015. Chany Lake (West Siberia) Environmental Profile. Academic Publishing House "Geo", Novosibirsk, pp. 19-33 (In Russian with English summary).

Khazin, L.B., Khazina, I.V., Krivonogov, S.K., Kuzmin, Ya.V., Prokopenko, A.A., Yi, S., Burr, G.S.,, 2016. Holocene climate changes in southern West Siberia based on ostracod analysis. Rus. Geol. Geoph. 57, 574–585.

Kirillov, V.V., Bezmaternykh, D.M., Dvurechenskaya, S.Y., Yermolaeva, N.I., Kirillova, T.V., Kovalevskaya, N.M., Marusin, K.V., Mitrofanova, E.Y., Romanov, R.E., Yurlova, N.I., 2015. Chapter 5. Limnology of Lake Chany. In: Vasiliev, O.F., Veen, J. (Eds.), 2015. Chany Lake (West Siberia) Environmental Profile. Academic

Publishing House "Geo", Novosibirsk, pp. 78-116 (In Russian with English summary).
Komatsu, G., Brantingham, P.J., Olsen, J.W., Baker, V.R., 2001. Paleoshoreline geomorphology of Boon Tsagaan Nuur, Tsagaan Nuur and Orog Nuur: the valley of lakes. Mongolia. Geomorph. 39, 83–98.
Korolyuk, A.Y., Kipriyanova, L.M., Drost, H.J., Kovalevskaya, N.M., Hanganu, J., Grigoras, I., 2015. Chapter 6. Vegetation of Chany Lake Region. In: Vasiliev, O.F., Veen, J. (Eds.), 2015. Chany Lake (West Siberia) Environmental Profile. Academic Publishing House "Geo", Novosibirsk, pp. 117-135 (In Russian with English summary).
Kosareva, L.R., Shcherbakov, V.P., Nurgaliev, D.K., Nurgalieva, N.G., Sycheva, N.K., Antonenko, V.V., Kuzina, D.M., Evtyugin, V.G., 2022. Periodization of Holocene climatic cycles based on synchronous variations in the magnetic and geochemical parameters of the sediments of Lake Bol'shoe Yarovoe (southwestern Siberia). Russ. Geol. Geoph. 61 (7), 723–737.
Krivonogov, S.K., Leonova, G.A., Mal'tsev, A.E., Bobrov, V.A., 2013. Stratigraphy and age of sapropels in lakes of southern West Siberia. In: Sedimentary Basins and Sedimentation and Post-Sedimentation Processes in Geological History: Proceedings VII All-Russian Lithological Conference (October 28–31, 2013). INGG SB RAS, Novosibirsk, Vol. 2, pp. 102–105 (In Russian).
Krivonogov, S., Gusskov, S., Khazin, L., 2008. A Holocene connection between the Aral-Caspian Basin and south West Siberia evidenced by aquatic microfauna: probable paleogeographic scenarios. Bull. Tethys Geol. Soc. Cairo 3, 11–18.
Krivonogov, S.K., Takahara, H., Yamamuro, M., Preis, Y.I., Khazina, I.V., Khazin, L.B., Safonova, I.Y., Ignatova, N.V., 2012a. Regional to local environmental changes in southern Western Siberia: evidence from biotic records of mid to late Holocene sediments of Lake Beloye. Palaeogeogr., Palaeoclim. Palaeoecol. 331–332, 177–193.
Krivonogov, S.K., Yamamuro, M., Takahara, H., Kazansky, A.Y., Klimin, M.A., Bobrov, V.A., Safonova, I.Y., Phedorin, M.A., Bortnikova, S.B., 2012b. An abrupt ecosystem change in Lake Beloye, southern Western Siberia: palaeoclimate versus local environment. Palaeogeogr., Palaeoclim. Palaeoecol. 331–332, 194–206.
Krivonogov, S.K., Burr, G.S., Kuzmin, Y.V., Gusskov, S.A., Kurmanbaev, R.K., Kenshinbay, T.I., Voyakin, D.A., 2014. The fluctuating Aral Sea: a multidisciplinary-based history of the last two thousand years. Gondwana Res. 26, 284–300.
Krivonogov, S., Kazansky, A., Khazin, L., Lui, Zh., Rudaya, N., Zhilich, S., Zhdanova, A., 2015a. Environmental history of Lake Chany, southern Western Siberia, in: Abstract for the XIX INQUA Congress Quaternary Perspectives on Climate Change, Natural Hazards and Civilization (26 July–2 August, 2015), Nagoya.
Krivonogov, S., Zhilich, S., Gusev, V., 2015b. New data on lake evolution in northern Central Asia, in: Abstract for the 13th International Paleolimnology Symposium (August 4–7, 2015). Lanzhou University, Lanzhou, p. 61.
Krivonogov, S.K., Gusev, V.A., Parkhomchuk, E.V., Zhilich, S.V., 2018. Intermediate lakes of the Chulym and Kargat river valleys and their role in the evolution of the Lake Chany basin. Rus. Geol. Geoph. 59, 541–555.
Last, W.M., Ginn, F.M., 2005. Saline systems of the Great Plains of western Canada: an overview of the limnogeology and paleolimnology. Saline Systems 1, 10. https://doi.org/10.1186/1746-1448-1-10.
Last, W.M., 1990. Lacustrine dolomite—an overview of modern, Holocene, and Pleistocene occurrences. Earth Sci. Rev. 27, 221–263.
Leeder, M., 1982. Sedimentology: Process and Product. Allen & Unwin, London.
Lehmkuhl, F., Grunert, J., Hülle, D., Batkhishig, O., Stauch, G., 2018. Paleolakes in the Gobi region of southern Mongolia. Quat. Sci. Rev. 179, 1–23.
Maltsev, A.E., Leonova, G.A., Bobrov, V.A., Krivonogov, S.K., 2019. Geochemistry of Holocene Sapropels from Small Lakes of the Southern Western Siberia and Eastern Baikal Regions. Academic Publishing House "Geo". Novosibirsk (In Russian.
Maltsev, A.E., Leonova, G.A., Bobrov, V.A., Krivonogov, S.K., Miroshnichenko, L.V., Vossel, Y.S., Melgunov, M.S., 2020. Geochemistry of carbonates in small lakes of southern West Siberia exampled from the Holocene sediments ofLake LAKE Itkul'. Rus. Geol. Geoph. 61 (3), 378–399. In Russian with English abstract.
Matasova, G.G., Kazansky, A.Y., Pozdnyakova, O.A., 2016. The Experience of Using the Rock Magnetic Methods for Assessing the Prospects of Magnetic Exploration in the Territory of Archaeological Monuments of the Barabinsk Forest Steppe. Izvestiya, Phys. Solid. Earth 52 (6), 869–883.
Mischke, S., Zhang, C., Plessen, B., 2020. Lake Balkhash (Kazakhstan): Recent human impact and natural variability in the last2900 years. J. Great Lakes Res. 46 (2), 267–276.
Nazarova, L., Bleibtreu, A., Hoff, U., Dirksen, V., Diekmann, B., 2017. Changes in temperature and water depth of a small mountain lake during the past 3000 years in Central Kamchatka reflected by chironomid record. Quat. Int. 447, 46–58.
Nechiporenko, G.O., Bondarenko, G.P., 1988. Conditions of Formation of Marine Carbonates. Nauka, Moscow (in Russian).
Riedel, F., Kossler, A., Tarasov, P., Wunnemann, B., 2011. A study on Holocene foraminifera from the Aral Sea and West Siberian lakes and its implication for migration pathways. Quat. Int. 229, 105–111.
Rudaya, N., Nazarova, L., Nourgaliev, D., Palagushkina, O., Papin, D., Frolova, L., 2012. Middle-Late Holocene environmental history of Kulunda, southwestern Siberia: vegetation, climate and humans. Quat. Sci. Rev. 48, 32–42.
Rudaya, N., Krivonogov, S., Słowinski, M., Cao, X., Zhilich, S., 2020. Postglacial history of the Steppe Altai: Climate, fire and plant diversity. Quat. Sci. Rev. 249, 106616.
Savkin, V.M., Orlova, G.A., Kondakova, O.V., 2006. The present day water balance of undrained Lake Chany. Geogr. Nat. Res. 1, 123–131. In Russian with English summary.
Savkin, V.M., Orlova, G.A., Vasiliev, O.F., Dvurechenskaya, S.Y., Kondakova, O.V., Saprykina, Y.V., Kuskovsky, V.S., 2015. Chapter 4. Hydrology. In: Vasiliev, O.F., Veen, J. (Eds.), 2015. Chany Lake (West Siberia) Environmental Profile. Academic Publishing House "Geo", Novosibirsk, pp. 42-77 (In Russian with English summary).
Selegei, V.V., 2015. Chapter 3. Climate. In: Vasiliev, O.F., Veen, J. (Eds.), 2015. Chany Lake (West Siberia) Environmental Profile. Academic Publishing House "Geo", Novosibirsk, pp. 34-41 (In Russian with English summary).
Shao, Y., Gong, H., Elachi, C., Brisco, B., Liu, J., Xia, X., Guo, H., Geng, Y., Kang, S., Liu, C., Yang, Z., Zhang, T., 2022. The lake-level changes of Lop Nur over the past 2000 years and its linkage to the decline of the ancient Loulan Kingdom. J. Hydrol. Regional Studies 40, 101002.
Shnitnikov, A.V., 1950. Intra-Century Level Fluctuations of Steppe Lakes in West Siberia and Northern Kazakhstan and Their Dependence on Climate. Proceedings of Laboratory of Lake Science of the USSR Academy of Sciences, Vol. 1. Izd. Akad. Nauk SSSR, Moscow, Leningrad (In Russian).
Shnitnikov, A.V., 1976. Large lakes of Middle Region and some ways of its usage. In: Shnitnikov, A.V. (Ed.), Lakes of Middle Region. Institute of limnology, Leningrad (In Russian).
Smirnova, N.P., Shnitnikov, A.V. (Eds.), 1982 Pul'siruyushchee ozero Chany (Pulsating Lake Chany) Nauka, Leningrad (In Russian).
Song, M., Zhilich, S., Krivonogov, S., Lin, Zh., 2015. Biomarkers based reconstructions of climatic changes from the Yarkov basin of Lake Chany, south Western Siberia, during the middle to late Holocene, in: Abstract for the 13th Int. Paleolimnology Symp. (August 4–7, 2015). Lanzhou University, Lanzhou, pp. 122–123.
Song, M., 2016. Hydrological changes in Asian inland since late Pleistocene and climatic implications of interactions between westerlies and East Asian summer monsoon. University of Hong Kong. Hong Kong SAR, China. PhD thesis..
Stief, P., Nazarova, L., De Beer, D., 2005. Chimney construction by Chironomus riparius larvae in response to hypoxia: microbial implications for freshwater sediments. J. North Amer. Benthol. Soc. 24 (4), 858–871.
Talbot, M.R., 1990. A review of palaeohydrological interpretation of carbon and oxygen isotopic ratios in primary lacustrine carbonates. Chem. Geol. (Isotope Geoscience Section) 80, 261–279.
Tarasov, P.E., Pushenko, M.Ya., Harrison, S.P., Saarse, L., Andreev, A.A., Leshinskaya, Z.V., Davydova, N.N., Dorofeyuk, N.I., Efremov, Yu.V., Elina, G.A., Elovicheva, Ya. K., Filimonova, L.V., Gunova, V.S., Khomutova, V.I., Kvavadze, E.V., Neustrueva, I. Yu., Pisareva V.V., Sevastyanov, D.V., Shelekhova, T.S., Subetto, D.A., Uspenskaya, O.N., Zernitskaya, V.P., 1996. Lake Status Records from the Former Soviet Union and Mongolia. Documentation of the Second Version of the Database, in: NOAA Paleoclimatology Publications Series. Report 5. World Data Center-A for Paleoclimatology.
Vasiliev, O.F., Veen, J. (Eds.), 2015. Chany Lake (West Siberia) Environmental Profile. Academic Publishing House "Geo". Novosibirsk (In Russian with English summary.
Veizer, J., 1983. Trace elements and isotopes in sedimentary carbonates. In: Reeder, R.J. (Ed.), Carbonates: Mineralogy and Chemistry. Rev. Mineral., Mineralogical Society of America, Washington, Vol. 11, pp. 265–299.
Yu, K., Lehmkuhl, F., Diekmann, B., Zeeden, C., Nottebaum, V., Stauch, G., 2017. Geochemical imprints of coupled paleoenvironmental and provenance change in the lacustrine sequence of Orog Nuur, Gobi Desert of Mongolia. J. Paleolimn. 58, 511–532.
Zhdanova, A.N., Solotchina, E.P., Solotchin, P.A., Krivonogov, S.K., Danilenko, I.V., 2017. Reflection of Holocene climatic changes in mineralogy of bottom sediments from Yarkovsky Pool of Lake Chany (southern West Siberia). Rus. Geol. Geoph. 58 (6), 692–701.
Zhdanova, A.N., Solotchina, E.P., Krivonogov, S.K., Solotchin, P.A., 2019. Mineral Composition of the Sediments of Lake Malye Chany as an Indicator of Holocene Climate Changes (Southern West Siberia). Rus. Geol. Geoph. 60 (10), 1163–1174.
Zhilich, S., Rudaya, N., Krivonogov, S., 2015. The Holocene environmental changes in the arid and semiarid regions of West Siberia inferred from lacustrine sediments. In: Abstract for the 13th Int. Paleolimnology Symposium (August 4–7, 2015). Lanzhou University, Lanzhou, pp. 62–63.
Zhilich, S.V., Rudaya, N.A., Nazarova, L.B., Palagushkina, O.V., Krivonogov, S.K., 2015a. Changes in Lake Chany and surrounding landscapes in the second half of the Holocene. In: Problems of Archeology, Ethnography, Anthropology of Siberia and Adjacent Areas: Proceedings Scientific Session of the Institute of Archeology and Ethnography SB RAS for 2015. Institute of Archeology and Ethnography SB RAS, Novosibirsk, pp. 232–236 (In Russian).
Zhilich, S.V., Rudaya, N.A., Krivonogov, S.K., 2016. Changes in vegetation and climate in the area of Lake Malye Chany in the late Holocene. Dinamika Okruzhayushchei Sredy i Global'nykh Izmenenii Klimata 13 (1), 68–75 (In Russian).
Zhilich, S., Rudaya, N., Krivonogov, S., Nazarova, L., Pozdnyakov, D., 2017. Environmental dynamics of the Baraba forest-steppe (Siberia) over the last 8000 years and their impact on the types of economic life of the population. Quat. Sci. Rev. 163, 152–161.
Zhilich, S.V., 2015. Palynological study of Lake Chany. In: Proceedings of "Trofimuk Readings" All-Russian Scientific Conference of Young Scientists (October 13–16, 2015). Novosibirsk, pp. 37–39 (In Russian).
Zhilich, S.V., 2019. Vegetation and Climate of Middle and Late Holocene in the South-West Western Siberia by Palynological Data. Novosibirsk. Autoreferat of PhD thesis (In Russian).